

University of Nevada

Reno

Wallrock Alteration, Vein Structure,
and Preliminary Fluid-Inclusion Studies,
Gooseberry Mine, Storey County, Nevada

A thesis submitted in partial fulfillment of the
requirements for the degree of Master of Science

by

Terry Ann Sprecher

11

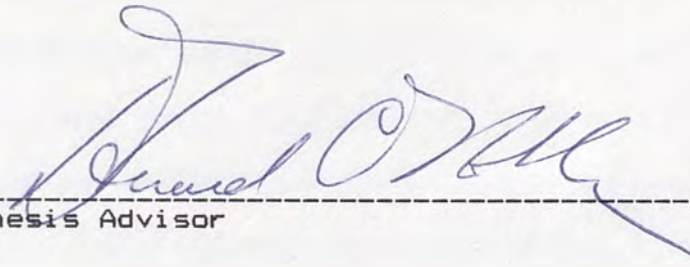
August, 1985

MINES
LIBRARY

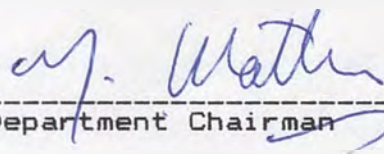
Thesis

2014

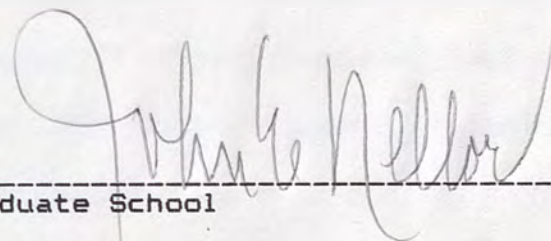
The thesis of Terry Ann Sprecher is approved:



Thesis Advisor



Department Chairman



Dean, Graduate School

University of Nevada

Reno

© 1985
Terry Ann Sprecher
431 Alpha Avenue
August, 1985

ACKNOWLEDGEMENTS

This thesis would not have been possible without the permission and cooperation of Asamera Minerals (U.S.) Inc.. I would like to thank Asamera for access to the Gooseberry Mine and pertinent data, for providing base maps, assay data, and miscellaneous supplies, and for providing blue-line copies of the finished plates. Special thanks go to Dr. Peter Clarke of the exploration branch of Asamera for assistance in shaping the proposal, for helpful discussions throughout the project, and for editing of the manuscript; to Jack Glynn, assistant mine geologist in 1983, for help in underground orientation and in sampling the inactive levels of the mine; to Rick Karlson, present mine geologist, for his interest, enthusiasm, and cooperation; and to the miners who helped make my first underground mapping project a pleasant experience.

My deepest gratitude goes to Dr. Larry Buchanan, of Fischer-Watt Mining Co. Inc., for suggesting the thesis project, for assistance, advice and encouragement throughout the project, and for serving on the thesis committee. Special thanks are extended to Dr. Donald Noble, committee chairman, for his assistance and critical comments, especially during the manuscript stage, and to Dr. Liang-Chi Hsu and Dr. Arthur Baker III, for serving as committee members.

My warmest thanks are also due to the following individuals and companies for their contributions to this project. Exploration Research Laboratories, Salt Lake City, Utah, along with C. Gary Clifton, provided complimentary gas analyses of the vein samples. Geothermal Development Associates and United Mining Corporation each permitted use of their diazo machines for working copies of the plates. Fischer-Watt Mining Co. Inc. kindly allowed the use of their drafting equipment. Dr. Tom Lugaski explained the mysteries of Wordstar to me. Special thanks are extended to John McCormack for instruction in X-ray diffraction techniques; to Doug Bruha and Dale Finn for instruction and advice in fluid-inclusion techniques; and to Dr. Don Hudson for countless discussions regarding wall-rock alteration. I would like to thank my fellow graduate students for their support, encouragement, and stimulating discussions, both in regards to this thesis and to geology in general. Lastly, I wish to thank my husband, Jonathan, for all of his encouragement, support, and suggestions, both geological and otherwise, without which this undertaking would have proven much more difficult.

ABSTRACT

The Gooseberry vein is a precious-metal, epithermal, calcite-quartz vein deposited in Tertiary volcanics along the east-west trending Gooseberry fault. Propylitized rocks envelop this fault and the north-northeast trending Red Top structures. The alteration pattern suggests that the Red Top structures may contain precious-metal mineralization at depth.

Ore-shoot location is controlled by abrupt change in dip, major change in strike, and intersection with northeast-trending faults. The silver-to-gold ratio increases markedly with depth.

Preliminary fluid-inclusion studies indicate a temperature of deposition between 240 and 245°C, probably under non-boiling conditions and hydrostatic pressure.

Additional chemical parameters have been extrapolated from alteration mineralogy, fluid-inclusion data, and mineral stability relationships. The estimated pH range is 5.53 to 6.16; O_2 fugacity range, $10^{-32.3}$ to $10^{-35.8}$ atmospheres; total sulfur range, 10^{-2} to $10^{-2.5}$ moles; and CO_2 range, 0.04 to 0.18 mole percent. The lower limit of mineralization is between 1350 and 1900 feet below the paleo-surface.

TABLE OF CONTENTS

ACKNOWLEDGEMENTS	ii
ABSTRACT	iv
LIST OF ILLUSTRATIONS.	vii
INTRODUCTION	1
LOCATION AND PHYSIOGRAPHIC FEATURES.	2
PREVIOUS WORK.	4
MINE HISTORY	4
REGIONAL GEOLOGY	6
GEOLOGY OF THE GOOSEBERRY MINE	10
STRATIGRAPHY	10
STRUCTURE.	12
VEIN MINERALOGY.	15
AGE OF MINERALIZATION.	18
WALL ROCK ALTERATION	20
INTRODUCTION	20
PROPYLITIC ASSEMBLAGE.	23
Propylitic Type P1.	23
Propylitic Type P2.	26
SMECTITE-QUARTZ ASSEMBLAGE	27
ILLITE-QUARTZ ASSEMBLAGE	28
DICKITE-SILICA ASSEMBLAGE.	28
SILICIFICATION	29
HORIZONTAL ZONATION OF HYDROTHERMAL ALTERATION ASSEMBLAGES	30
Adjacent to the Gooseberry Vein	30
Adjacent to the Red Top Structures.	30
VERTICAL ZONATION OF HYDROTHERMAL ALTERATION ASSEMBLAGES	31
SUPERGENE ALTERATION	31
VARIATIONS IN THE ATTITUDE, THICKNESS, AND METAL CONTENT OF THE GOOSEBERRY VEIN	33
INTRODUCTION	33
LONGITUDINAL PROJECTION OF THE RECONSTRUCTED GOOSEBERRY VEIN SHOWING STRUCTURE CONTOURS	34
LONGITUDINAL PROJECTION OF THE RECONSTRUCTED GOOSEBERRY VEIN SHOWING VEIN THICKNESS CONTOURS	35
PRECIOUS-METAL MINERALIZATION.	37
Longitudinal Projection of the Reconstructed Gooseberry Vein Showing Gold Assay Contours	37
Longitudinal Projection of the Reconstructed Gooseberry Vein Showing	

TABLE OF CONTENTS (CONT)

Figure	Silver Assay Contours	38
	Longitudinal Projection of the Reconstructed Gooseberry Vein Showing Silver-to-Gold Ratio Contours	38
	Longitudinal Projection of the Reconstructed Gooseberry Vein Showing Equivalent-Silver-Foot Contours	39
	FLUID-INCLUSION STUDIES.	42
	INTRODUCTION	42
	SAMPLE DESCRIPTIONS.	42
	BOILING VERSUS EFFERVESCENCE	45
	HOMOGENIZATION TEMPERATURES.	49
	SALINITY ESTIMATE.	49
	GAS ANALYSES	51
	DEPTH OF MINERALIZATION.	58
	CHEMICAL PARAMETERS DURING ORE DEPOSITION.	61
	PARAMETERS AT DEPTH.	61
	Estimated Carbon Dioxide Content.	61
	Estimated pH.	65
	Estimated Oxygen Fugacity	65
	Estimated Total Sulfur.	67
	PARAMETERS AT THE SURFACE.	68
	DISCUSSION	71
	APPENDICES	76
	APPENDIX A: FIELD TECHNIQUES.	76
	APPENDIX B: X-RAY EQUIPMENT AND SAMPLE PREPARATION METHODS	77
	APPENDIX C: SELECTED THIN-SECTION AND X-RAY DIFFRACTION DATA.	77
	APPENDIX D: METHODS UTILIZED IN CONSTRUCTING THE STRUCTURE CONTOUR PROJECTION AND ACCOMPANYING OVERLAYS	81
	APPENDIX E: HEATING-FREEZING EQUIPMENT AND FLUID-INCLUSION SAMPLE PREPARATION METHODS	84
	APPENDIX F: GAS ANALYSIS EQUIPMENT AND SAMPLE PREPARATION METHODS	85
	APPENDIX G: SAMPLE CALCULATIONS	86
	REFERENCES	88

LIST OF FIGURES

Figure 1.	Location map of the Gooseberry mine and other districts in western Nevada.	3
2.	Generalized stratigraphic section near the Gooseberry mine.	7
3.	Simplified geologic and alteration map of the Gooseberry mine claim block	11
4.	Paragenesis of the Gooseberry vein. . .	17
5.	Diagrammatic representation of left-lateral strike-slip and dip-slip movement along the Gooseberry fault . .	36
6.	Composite histogram of homogenization temperatures.	50
7.	Total C/total S - total oxidized (C + S)/total reduced (C + S) of analyzed volatiles	57
8.	Depth - carbon dioxide content at a salinity of 2 eq. wt. % NaCl.	62
9.	The stability of Ca-aluminum silicates as a function of carbon dioxide and temperature	64
10.	Solution pH - temperature relations constrained by the Kspar-Kmica-quartz equilibrium at 3 salinities	64
11.	Log oxygen fugacity - 1/T diagram showing typical oxidation reactions among minerals.	66
12.	Interpretive cross section showing the alteration types present at the Gooseberry mine	72

LIST OF TABLES

Table	1.	Summary of the alteration types present at the Gooseberry mine and their diagnostic minerals	21
	2.	Summary of criteria for primary origin of fluid inclusions.	44
	3.	Summary of evidence for rapid precipitation of vein material by boiling at the Gooseberry mine.	47
	4.	Homogenization temperature range and median.	50
	5.	Salinity ranges resulting from fluid-inclusion studies of various epithermal, volcanic-hosted, precious-metal, low-sulfide, vein deposits	52
	6.	Gas analysis data from fluid-inclusion samples from the Gooseberry vein	54
	7.	Weight ratios of analyzed volatiles	57
	8.	Estimated mole percent of carbon dioxide	62
VIIIa		Longitudinal projection of the reconstructed Gooseberry vein showing Silver-Gold Ratio Contours.	77
VIIIb		Longitudinal projection of the reconstructed Gooseberry vein showing Silver-to-Gold Ratio Contours.	78
VIIIc		Longitudinal projection of the reconstructed Gooseberry vein showing Sulfur-to-Silver-Ratio Contours.	79

LIST OF PLATES

Plate	I	Geologic Map of the Gooseberry Mine Claim Block, Storey County, Nevada.	in pocket
	II	Surface Alteration Map of the Gooseberry Mine Claim Block, Storey County, Nevada.	"
	III	Alteration Map of the 100, 200, 400, 500, 800, 1000, 1150, and 1300 Levels of the Gooseberry Mine	"
	IV	Longitudinal Projection of the Gooseberry Mine Workings.	"
	V	Longitudinal Projection of the Reconstructed Gooseberry Vein Showing Structure Contours.	"
	VI	Composite Plan and Cross Sections of the Reconstructed Gooseberry Vein	"
	VII	Longitudinal Projection of the Reconstructed Gooseberry Vein Showing Vein Thickness Contours	"
	VIIIa	Longitudinal Projection of the Reconstructed Gooseberry Vein Showing Gold Assay Contours	"
	VIIIb	Longitudinal Projection of the Reconstructed Gooseberry Vein Showing Silver Assay Contours	"
	IXa	Longitudinal Projection of the Reconstructed Gooseberry Vein Showing Silver-to-Gold Ratio Contours.	"
	IXb	Longitudinal Projection of the Reconstructed Gooseberry Vein Showing Equivalent-Silver-Foot Contours.	"

INTRODUCTION

The Gooseberry mine is an epithermal silver-gold mine located in western Nevada. Ore is hosted by a calcite-quartz vein with wall rocks of the Kate Peak Formation, a Tertiary volcanic unit composed predominantly of dacite and rhyodacite lava flows. Approximately one-half mile of the strike length of the vein has been developed to a depth of approximately 1150 feet (see Mine History section, below). Propylitized volcanic rocks envelop the explored sections of the Gooseberry vein; propylitized and argillized rocks are exposed elsewhere on the property. Prior to the start of this project, the nature and distribution of the altered rocks had not been mapped in detail.

The primary objective of this study was to develop an exploration model that would facilitate the discovery of additional ore shoots. To accomplish this, the following techniques were employed: construction of large-scale surface and underground alteration maps, construction of a vein structure contour map with accompanying thickness and assay overlay maps, and nondestructive and destructive fluid inclusion study.

Intensely propylitized to propylitized rocks envelop the major east-west and north-northeast trending structures at the Gooseberry mine, thus enabling these

structures to be identified and mapped at the surface. The alteration pattern suggests that the Red Top east and west structures may also be mineralized. Ore shoot location along the exposed section of the Gooseberry vein was controlled partially by the shape of the Gooseberry fault zone prior to mineralization and partially by the intersection of the north-northeast trending fault set with the Gooseberry fault zone.

LOCATION AND PHYSIOGRAPHIC FEATURES

The Gooseberry mine is located in Storey County, Nevada, approximately 24 miles east of Reno (Fig. 1). The mine is situated in the Virginia Range, in Sections 25, 26, and 36, Township 19N, Range 22E. Elevation of the claim block ranges from 5200 feet to 6600 feet. The climate in western Nevada is arid to semiarid; average rainfall fluctuates from 5 to 10 inches per year. Summer temperatures often exceed 90° F, whereas winter temperatures generally drop below 32° F. The vegetation is typical of this part of Nevada. Sage, salt grass, shadscale, and greasewood are common at lower elevations; piñon pine and juniper dominate at higher elevations.



Fig. 1. Location map of the Gooseberry mine and other districts in western Nevada (modified from Moore, 1969).

PREVIOUS WORK

Only a few publications refer to the Gooseberry mine. The most informative discussions on geology are those of Rose (1969), Bonham (1969), and Stewart (1980). A small number of unpublished reports (R. Hardyman, undated; S. Kleeberger, undated; Kemp, 1976) discuss the geology and structure of the claim block, as well as the ore and gangue mineralogy. Schafer (1976) studied the geology and structure of the claim block and the vein mineralogy, and briefly described the wall-rock alteration. Morton et al. (1977) reported a K-Ar age of 10.3 ± 0.3 m. y. on vein material. Zerwick (1982) utilized altered rock from the Gooseberry mine in a study of adsorbed gases and clay minerals. Asamera Minerals (U.S.) Inc. (Anonymous, 1983) has printed a short brochure that summarizes the mine history, geology, and current operations. Royse (in preparation) is completing a soil geochemistry study of the area overlying the vein and of the intensely altered area to the south.

MINE HISTORY

The Gooseberry vein was discovered between 1904 and 1906 by an unidentified prospector from the nearby Ramsey district. The property was acquired in 1910 by an unknown

miner who sank a 50 foot shaft by hand and excavated a few shallow trenches. In 1928, J. D. Martin Sr. purchased half of the mining rights and by the mid 1930's the Martin family completely controlled the district. The Martin family sank a 1000 foot deep inclined shaft and developed over 9000 feet of drifts, but never produced any ore.

APCO Minerals, Inc. acquired the property in 1974. A 1450 foot vertical shaft was constructed and a 350 ton per day mill was partially built. In 1976, APCO Minerals, Inc. sold the mine to Westcoast Oil and Gas Corporation. The latter completed the mill, installed a tailings pond, and began production. In the spring of 1982, the Gooseberry mine was shut down and put up for sale. Asamera Minerals (U.S.) Inc. purchased the mine in late 1982 and resumed production in August of 1983 (Anonymous, 1983). As of December 31, 1984, Asamera Inc. reported proven and probable ore reserves of 216,505 short tons with an average grade of 0.209 oz/ton gold and 8.08 oz/ton silver (Asamera Inc., 1984). In 1984, 97,435 tons of ore were produced, yielding 617,733 ounces of silver and 14,938 ounces of gold.

REGIONAL GEOLOGY

The oldest rocks exposed in the Virginia Range are Triassic and Jurassic metavolcanic and metasedimentary rocks of the Peavine Sequence (Bonham, 1969). These are intruded in a few localities by Cretaceous plutonic rocks that range in composition from granite to quartz diorite (Bonham, 1969; Rose, 1969). No Mesozoic rocks are exposed within the Gooseberry mine claim block; the nearest outcrops of both the Peavine Sequence and the Cretaceous intrusives are located just east of the Ramsey district (Rose, 1969; Fig. 1).

The Mesozoic rocks are unconformably overlain by Tertiary and Quaternary volcanic and sedimentary rocks with an estimated maximum total thickness of 14,000 feet (Rose, 1969; Bonham, 1969; Fig. 2). The "Hartford Hill Formation" has been divided into several units (Bingler, 1973; Wallace, 1975; Proffett and Proffett, 1976; and Bingler, 1978) and the name "Hartford Hill Formation" has been abandoned (Bingler, 1978). However, the northern Virginia Range has not been remapped, and it is uncertain what formation name to assign to the rocks that Rose (1969) named the Hartford Hill Formation.

The Kate Peak Formation hosts mineralization at the Gooseberry mine, as well as at the nearby Ramsey and Talapoosa districts. This formation is composed mainly of

Age	Unit	Lithology	Approx. Max. Thickness
Holocene	Alluvium	Gravel, sand, silt.	50'
	Lake Lahontan deposits	Sand, silt, gravel.	125'
Pleistocene	Older Alluvium	Gravel, sand.	35'
	McClellan Peak Basalt	Olivine basalt flows, cinders.	35'
	Mustang Andesite	Hornblende-pyroxene trachyandesite flows.	350'
	Lousetown Formation	Basalts, andesites, and trachyandesites—mostly lava flows—some intrusives.	350'
Unconformity			
	Knickerbocker (?) Andesite	Pyroxene andesite dikes and plugs.
	Coal Valley Formation	Sandstone, rhyolite tuff, shale, diatomite.	500'
	Kate Peak Formation	Dacite and rhyodacite flows, flow breccias, some interbedded rhyolite tuff, diatomite. Dacitic to rhyolitic intrusives.	1500'
Unconformity			
Miocene	Desert Peak Formation	Upper: sandstone, shale, and diatomite. Lower: dacite and rhyodacite flows and flow breccias.	3000'
	Chloropagus Formation	Basaltic and andesitic flows with interbedded rhyolitic tuffs and sediments. Basaltic intrusives.	3000'
Unconformity			
	Old Gregory Formation	Mainly rhyolitic tuffs, some shale and andesitic lava.	1200'
	Alta Formation	Andesitic and basaltic lavas, breccias, and intrusives.	1000'
	"Hartford Hill Formation"	Rhyolitic ash-flow tuffs.	2500'
Unconformity			
Oligocene	Pre-Hartford Hill Sediments	Olive green claystone.	300'
Unconformity			
Jurassic		Metamorphic, dioritic, and granitic rocks.	?

Fig. 2. Generalized stratigraphic section near the Gooseberry mine (modified from Rose, 1969). The age boundaries have been modified to reflect K-Ar ages for the McClellan Peak Basalt, Lousetown Formation, Coal Valley Formation, Kate Peak Formation, Chloropagus Formation, Alta Formation, and "Hartford Hill Formation" (Silberman and McKee, 1972), and for the Mustang Andesite (Morton et al., 1977). See text for discussion of the "Hartford Hill Formation".

dacite and rhyodacite lava flows and has a maximum thickness of about 1500 feet (Rose, 1969). Silberman and McKee (1972) have obtained two K-Ar age determinations on unaltered rocks of the Kate Peak Formation of 13.1 ± 0.8 and 12.7 ± 0.2 m. y. (recalculated using present constants, see Dalrymple, 1979).

In contrast to the north-northeast trending mountain ranges in the area, the Virginia Range trends east-west (Fig. 1). It is bounded on the north and south by northeast to east-northeast trending valleys (Bonham, 1969), and is tilted westward (Bonham, 1969) and slightly to the north (Moore, 1969). These differing structural trends can be explained by regional structural features.

The Virginia Range is located in the transitional zone between the Basin and Range province and the Sierra Nevada Mountains (Fig. 1). The Walker Lane, which is just east of the Virginia Range (Fig. 1), is a northwest-trending zone of an echelon, right-lateral strike-slip faults that extends from southern Nevada into northern California. The Walker Lane in southern Washoe County is a primary, first-order, right-lateral wrench fault (Bonham, 1969) with conjugate, northeast-trending, left-lateral strike-slip faults.

Two main deformational episodes are documented in the rocks of the Virginia Range. The earliest occurred in the late Mesozoic and resulted in folding, faulting, and low-

grade regional metamorphism of the Peavine Sequence (Bonham, 1969). The later episode commenced approximately 17 million years ago and is still active today (Stewart, 1980); this event produced the Basin and Range province. Repeated tilting and warping, accompanied by block faulting, occurred. Evidence of the progressive nature of this event is preserved in the rocks of the Virginia Range: pre-Kate Peak units are strongly folded; rocks of the Kate Peak and Coal Valley Formations are only weakly folded; and the Lousetown Formation exhibits minor tilting and faulting, but no folding (Rose, 1969). The folds and major faults near the Gooseberry vein and to the north trend approximately east-west, whereas the folds further south trend northeast-southwest and the major faults trend north-south (Rose, 1969).

Schafer (1976) observed that the Gooseberry mine lies in the center of a generally east-west trending zone of precious-metal mineralization defined by the Peavine, Wedekind, Ramsey, and Talapoosa districts (Fig. 1). Other nearby precious-metal districts include the Olinghouse and Comstock districts (Fig. 1).

GEOLOGY OF THE GOOSEBERRY MINE

STRATIGRAPHY

The Kate Peak Formation is the only Tertiary unit that is exposed at the Gooseberry mine site (Rose, 1969; Schafer, 1976). Within the area of investigation, the Kate Peak Formation consists primarily of dacite lava flows (Fig. 3, Plate I), but a local rhyodacite flow, a few lahars, a small intrusive, and an andesite flow are also present. Gravel of probable Pleistocene age and Quaternary alluvium unconformably overlies the Kate Peak Formation in the major drainages (Fig. 3, Plate I).

In the Virginia City area, the Kate Peak Formation has been divided into an upper and a lower member (Hudson, 1984a, b). The lower member is pervasively propylitized, whereas the upper member is relatively unaltered; the two members are nearly identical with regard to original minerals and textures (Hudson, 1984a). Pervasive propylitization does not occur at the Gooseberry mine, therefore, the Kate Peak Formation cannot be correlated with either the upper or the lower member as defined by Hudson (1984a, b).

The Kate Peak Formation is fresh in appearance over most of the study area (Fig. 3). The dacites are gray to reddish brown and contain abundant plagioclase and mafic

← Alta Formation?
OK

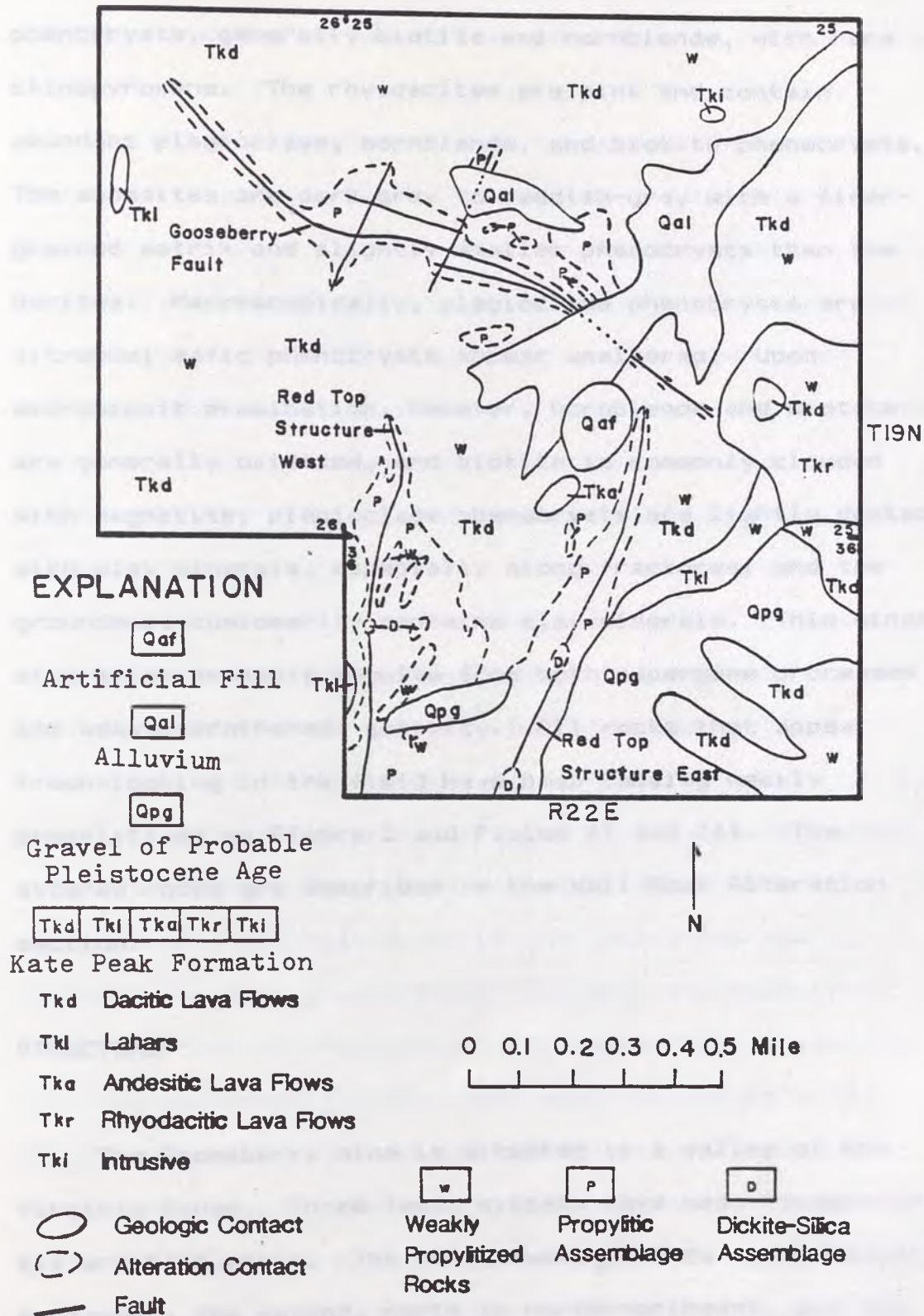


Fig 3. Simplified geologic and alteration map of the Gooseberry mine claim block.

phenocrysts, generally biotite and hornblende, with rare clinopyroxene. The rhyodacites are pink and contain abundant plagioclase, hornblende, and biotite phenocrysts. The andesites are dark gray to reddish-gray with a finer-grained matrix and slightly smaller phenocrysts than the dacites. Macroscopically, plagioclase phenocrysts are vitreous; mafic phenocrysts appear unaltered. Upon microscopic examination, however, hornblende and biotite are generally oxidized, and biotite is commonly clouded with magnetite; plagioclase phenocrysts are lightly dusted with clay minerals, especially along fractures; and the groundmass customarily contains clay minerals. This minor alteration probably results from both supergene processes and weak hydrothermal activity. All rocks that appear fresh-looking in the field have been labeled weakly propylitized on Figure 3 and Plates II and III. The altered rocks are described in the Wall Rock Alteration section.

STRUCTURE

The Gooseberry mine is situated in a valley of the Virginia Range. Three fault systems have been recognized; all are high angle. The first system trends approximately east-west, the second, north to north-northeast, and the third, north-northwest. The north-northwest fault set has

not been observed at the surface, and thus is not shown on Figure 3.

The Gooseberry fault trends approximately east-west across this valley near its northern boundary; the Gooseberry vein is located along the central section of the Gooseberry fault (Plate 1). Schafer (1976) has described this fault as normal with a left-lateral component of motion. This study has confirmed Schafer's interpretation (see Longitudinal Projection of the Reconstructed Gooseberry Vein Showing Vein Thickness Contours section, below).

The Gooseberry fault is enveloped on the surface by a zone of obviously propylitized rock that is less than 400 feet wide (Fig. 3, Plate II). Detailed mapping of alteration assemblages indicates the local presence of two subparallel, shorter, structures. One lies approximately 250 feet north of the Gooseberry vein, the other, approximately 200 feet south of the vein. The small, isolated zones of propylitized rock near the Gooseberry fault are probably associated with sympathetic structures.

Two small faults that trend north-northeast across the Gooseberry fault zone have been identified at the surface by the presence of propylitized rock (Fig. 3, Plate II). Both are expressed underground as zones of high-angle faults that trend north-northeast to northeast and cut the vein.

Numerous faults offset the vein at depth. The vast majority of these trend north-northwest. The largest of the offsets are shown on Plate III; most are too small to plot at this scale. Surface alteration patterns are not associated with the north-northwest trending faults.

Two north-south trending linear zones of alteration bound the southern Gooseberry basin near its western and eastern margins (Fig. 3, Plate II). The Red Top structure west may be a continuation of a high-angle fault that Rose (1969) shows as ending approximately one mile south of the study area, the west side of which has moved upward relative to the east side (Rose, 1969). The propylitic alteration enveloping the Red Top structure west cannot be identified further to the north than shown on Figure 3 and Plate II, in spite of moderately abundant outcrops. Therefore, the Red Top structure west probably terminates in the southwest quarter of section 25 (Fig. 3; Plate II) and does not intersect the Gooseberry fault.

The Red Top structure east (Fig. 3, Plate II) is probably a continuation of another high-angle fault that Rose (1969) shows as ending less than one-quarter mile south of the study area. The northern limit of this alteration zone could not be determined due to lack of outcrop (Plate II). However, given the change in structural grain from east-west to north-south (see Regional Geology section, above) and the likelihood that

the Red Top structure west does not intersect the Gooseberry fault, it may be surmised that the Red Top structure east also terminates before intersecting the Gooseberry fault.

Although the Gooseberry fault clearly predates mineralization, sections of the vein are brecciated, suggesting that movement has taken place after mineralization (Hardyman, undated). The north-northeast trending cross faults are probably younger than the Gooseberry fault; they displace the vein slightly. These faults are associated on the surface with altered rocks similar to those that occur along the Gooseberry fault, indicating that they, too, were open during at least part of the mineralizing event. Due to the nature of associated alteration, the Red Top structures are also suspected of having been open during the mineralizing event. The north-northwest trending fault set is the youngest of the three fault sets, and is post-mineralization. Underground, the north-northwest trending fault set is seen to offset both the north-northeast-trending set and the Gooseberry fault.

VEIN MINERALOGY

Vein mineralogy was not addressed in this study, partly due to the Gooseberry mine staff denying access to

the stopes, and partly because this subject has already been treated by Kemp (1976), Kleeberger (undated), and Schafer (1976).

The most abundant gangue mineral in the Gooseberry vein is calcite, followed by quartz, adularia, and hydrobiotite (interlayered biotite and vermiculite). The vein paragenesis, as presented by Kleeberger, is reproduced in Figure 4A. Calcite was deposited first, followed by four episodes of quartz deposition. Adularia was deposited during the second and third stage of quartz deposition, just prior to the ore minerals. Presumably, the term "ore minerals" refers to the minerals listed in Figure 4B, but this point is not clarified by Kleeberger (undated). Hydrobiotite was one of the last minerals to form.

The precious-metal minerals are associated with both quartz and calcite. Kleeberger's (undated) version of the base and precious-metal paragenesis (Fig. 4B) differs substantially from that of Schafer (Fig. 4C). It is unknown which version is the more correct.

The Gooseberry vein crops out in only one locality (Plate II). In outcrop, the vein is composed of white, coarse-grained calcite and is roughly six inches thick. Approximately 200 feet west of the vein outcrop is a small prospect pit that contains abundant, large chunks of calcite float (Plate II). Undoubtedly, the vein cropped

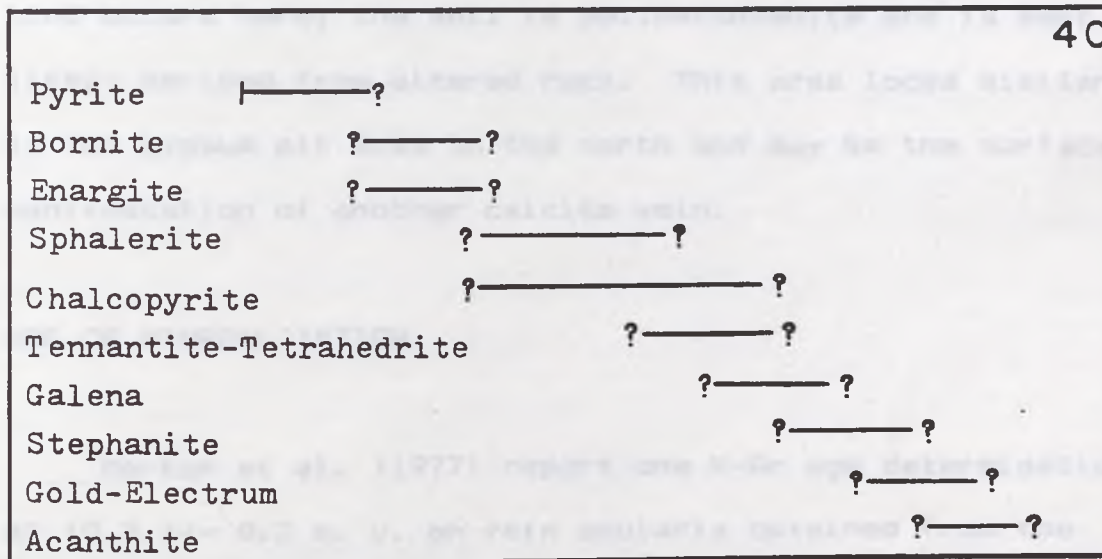
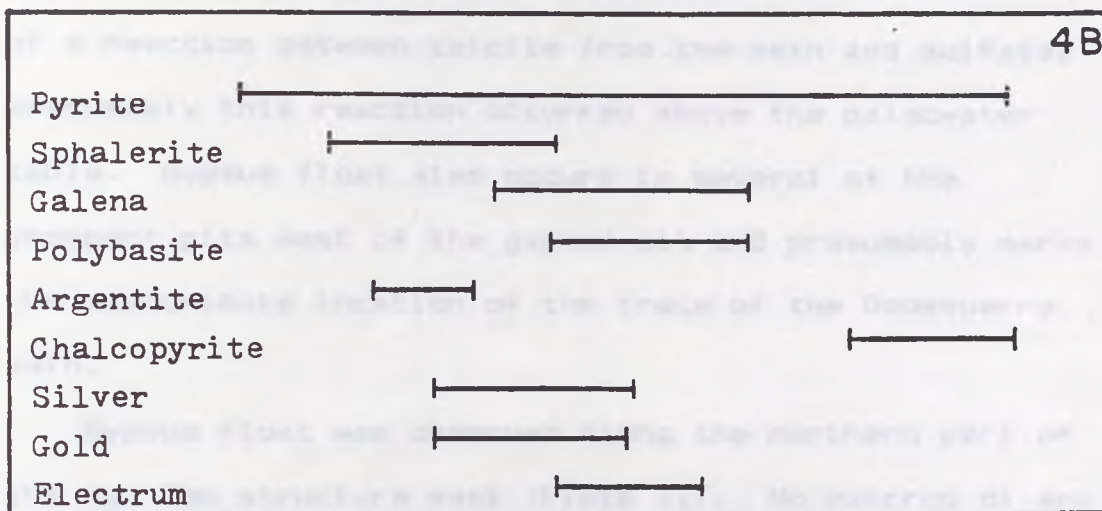
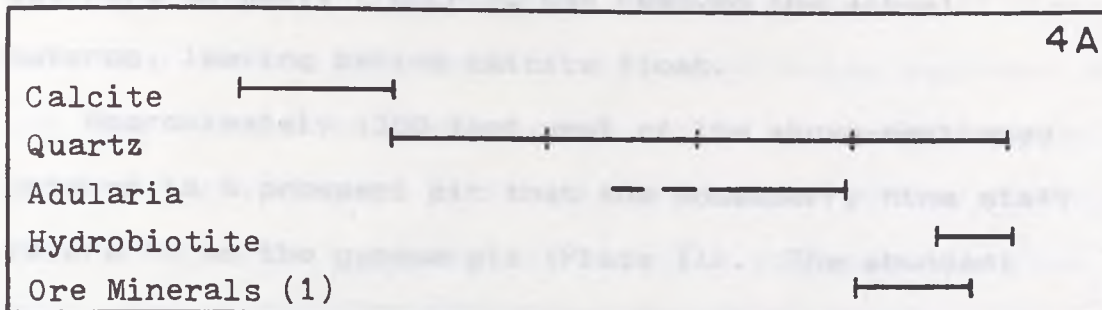


Fig. 4. Paragenesis of the Gooseberry vein. A. After Kleeberger (undated). (1) See text for explanation. B. Base- and precious-metal mineral paragenesis (after Kleeberger, undated). C. Base- and precious-metal mineral paragenesis (after Schafer, 1976).

out here as well; trenching has removed the actual outcrop, leaving behind calcite float.

Approximately 1300 feet west of the above-mentioned outcrop is a prospect pit that the Gooseberry Mine staff refers to as the gypsum pit (Plate II). The abundant gypsum float present here is probably the result of a reaction between calcite from the vein and sulfate; presumably this reaction occurred above the paleowater table. Gypsum float also occurs in several of the prospect pits west of the gypsum pit and presumably marks the approximate location of the trace of the Gooseberry vein.

Gypsum float was observed along the northern part of the Red Top structure east (Plate II). No outcrop of any kind occurs here; the soil is yellowish-white and is most likely derived from altered rock. This area looks similar to the gypsum pit area to the north and may be the surface manifestation of another calcite vein.

AGE OF MINERALIZATION

Morton et al. (1977) report one K-Ar age determination of 10.3 ± 0.3 m. y. on vein adularia obtained from the 1000 level of the Gooseberry mine. This date may be slightly older than the age of mineralization because adularia was deposited prior to the ore minerals (Fig. 4A).

TABLE 1. Summary of WALL ROCK ALTERATION
at the Gooseberry Mine and their diagnostic minerals.

Alteration Type	Diagnostic Minerals
-----------------	---------------------

INTRODUCTION

Surface and underground alteration mapping at the Gooseberry mine was conducted during the summer of 1983. Five distinct hydrothermal alteration assemblages were identified based upon outcrop appearance: the propylitic assemblage, the smectite-quartz assemblage, the illite-quartz assemblage, the dickite-silica assemblage, and silicification. X-ray diffraction analysis and thin-section examination verified the existence of these five assemblages and indicated that the propylitic assemblage could be further divided into two types, propylitic type P1 and propylitic type P2. Table 1 summarizes the six types of hydrothermal alteration that occur at the Gooseberry mine.

Unaltered-looking rocks of the Kate Peak formation are described in the Stratigraphy section, above. They are considered to have been only mildly affected, if at all, by the hydrothermal fluids, and thus are not included in this section. The effects of supergene alteration are discussed in the last part of this section.

Appendix A describes the field techniques utilized and lists the number of samples collected on the surface and underground. The locations of surface samples are shown

Table 1. Summary of the Alteration Types Present at the Gooseberry Mine and their Diagnostic Minerals.

Assemblages:	Propylitic		M	I	D-S	S
Types:	P1	P2				
smectite	D	D	D	-	-	+/-
illite	+/-	+/-	+/-	D	-	+/-
mixed layer-clays	+/-	+/-	+/-	-	-	+/-
chlorite	D	+/-	-	-	-	-
calcite	D	+/-	+/-	-	-	-
albite	D	-	-	-	-	+/-
adularia	D	-	-	-	-	+/-
epidote	D	+/-	-	-	-	+/-
clinozoisite	D	+/-	-	-	-	+/-
hematite	+	+/-	-	-	-	+/-
pyrite	+/-	-	-	-	-	+/-
quartz	+/-	+/-	D	D	+/-	D
zeolites	+/-	+/-	-	-	-	-
dickite	-	-	-	-	D	-
alunite	-	-	-	-	+/-	-
cristobalite	-	-	-	-	+/-	-
opal	-	-	-	-	+/-	-

Symbols: P1 = propylitic type P1; P2 = propylitic type P2; M = smectite-quartz assemblage; I = illite-quartz assemblage; D-S = dickite-silica assemblage; S = silicification; D = diagnostic mineral; + = mineral present; - = mineral absent; +/- = mineral present or absent.

on Plate II, of underground samples, on Plate III, and of fluid-inclusion samples, on Plate IV. Plate IV is a longitudinal projection of the Gooseberry mine workings as of August, 1983. Level numbers correspond with approximate depth, in feet, below the surface. "Old" levels were developed from the incline shaft; "new" levels were developed from the vertical shaft.

Phyllosilicate minerals were identified by X-ray diffraction techniques; thin-section study provided textural relationships and aided in the identification of less abundant mineral phases. The X-ray equipment and sample preparation methods utilized are described in Appendix B. Selected thin-section and X-ray diffraction data are tabulated in Appendix C.

The individual minerals of the chlorite group cannot be distinguished by X-ray diffraction methods (Grim, 1968); the term chlorite, as used herein, refers to the chlorite group of minerals. Likewise, the term smectite refers to the smectite family of minerals. Srodon and Eberl (1984) suggest that the term "illite" be reserved for "a non-expanding, dioctahedral, aluminous, potassium mica-like mineral which occurs in the clay-size fraction", and that the term "illitic material" refer to the "approximately ten angstrom component of the clay-size fraction". However, for simplicity's sake, the ten angstrom clay mineral discussed below will be referred to

as illite rather than as illitic material. The individual members of the kandite (kaolin) group can generally be distinguished by X-ray diffraction techniques (Grim, 1968; Appendix C). The presence of mixed-layer clays was demonstrated by glycolating and re-X-raying selected whole-rock samples.

PROPYLITIC ASSEMBLAGE

Propylitized rock is the most common type of altered rock at the Gooseberry mine (Fig. 3, Plate II); it surrounds the Gooseberry fault as well as both of the Red Top structures. Field criteria were utilized to define rocks of this assemblage. All volcanics that were greenish in outcrop were designated propylitized, as were all altered volcanics that contained recognizable plagioclase phenocrysts. The propylitic assemblage has been divided into two types based upon alteration mineralogy.

Propylitic Type P1

The propylitic type P1 is defined by the following association: smectite + chlorite + calcite + albite + adularia + epidote + clinozoisite. In addition, illite, mixed-layer clays, hematite, pyrite, quartz, stilbite,

and/or heulandite may be present.

Microscopically, individual plagioclase phenocrysts are greater than fifty percent altered. Calcite is the dominant replacement mineral, accompanied by adularia, albite, a minor amount of smectite and, in some rocks, illite, and/or traces of epidote or clinozoisite. Relict hornblende and biotite phenocrysts are commonly replaced by hematite, chlorite, and smectite, but illite, epidote, and/or calcite may also be present. The groundmass is customarily altered to smectite and may also contain chlorite, illite, calcite, pyrite, epidote, hematite, adularia, albite, and/or quartz.

Rocks of the propylitic type P1 have been subdivided into moderately propylitized and intensely propylitized rock based upon outcrop appearance (Plates II and III). In outcrop, moderately propylitized Kate Peak ranges from green to olive green; the plagioclase phenocrysts are dull, white, and gouge readily with a knife point. Intensely propylitized Kate Peak is off-white to light yellow to dark yellow-orange; remnant plagioclase phenocrysts are difficult to distinguish from the groundmass. Jarosite, goethite, and/or hematite are responsible for the yellow and orange color of the intensely propylitized rock.

Intensely propylitized rocks of the propylitic type P1, labeled (P1S) on Plates II and III, undoubtedly have

undergone some supergene oxidation, especially those at the surface. However, some of the P1S rocks do not contain iron oxides and do contain unoxidized pyrite. Therefore, the occurrence of P1S rocks can not be attributed solely to supergene processes.

As a rule, smectite, calcite, hematite, adularia, albite, epidote, and clinozoisite are ubiquitous throughout rocks of the propylitic type P1. Smectite decreases and chlorite increases with depth. The abundance of calcite and epidote/clinozoisite shows an inverse relationship. Hematite occurs in clots and microveinlets and decreases slightly toward the vein. At the 500 level and above, supergene hematite, jarosite, and/or goethite are present; it is impossible to distinguish between the supergene and hypogene hematite. Both albite and adularia decrease away from the vein.

Illite is generally not noticeable in X-ray diffraction patterns at the 1000 level, but occurs at and above the 800 level. It is ordinarily a very minor constituent of the P1 assemblage. Mixed-layer clays are not very common, but do occur (based on X-ray diffraction data).

Pyrite is common in the wallrock near the vein and progressively decreases away from the vein until it disappears. It occurs at all levels of the mine; pyrite casts are evident in the surface rocks near the vein.

Only two samples contained zeolites, one from the 1150 level, and one from the 1000 level. This is an insufficient sample population to confidently predict any zonation trends. Based on X-ray diffraction patterns, the zeolites appear to be stilbite and heulandite.

Propylitic Type P2

The most common mineral of the propylitic type P2 is smectite. Illite, mixed-layer clays, and zeolites may also occur, but are not common. One or two of the following minerals may be present in minor amounts: calcite, epidote, and chlorite.

Rocks of the propylitic type P2 are commonly off-white to yellowish in outcrop, but may also be light green. Plagioclase phenocrysts are dull, white, and gouge readily with a knife point.

Plagioclase phenocrysts are altered to smectite. They may contain minor calcite and/or illite, but not epidote, adularia, or albite. Oxybiotite phenocrysts are common. The groundmass is heavily altered, commonly to smectite, but calcite, epidote, zeolites, or chlorite may be present as well.

Smectite is ubiquitous throughout rocks of the P2 type. Illite is a minor constituent; the amount of illite appears to increase with increasing intensity of

alteration. Mixed-layer clays are not common, but can be recognized by X-ray diffraction techniques. Hematite is very common, but it is impossible to determine whether the hematite is supergene or hypogene in origin. Based on mineralogic similarities with P1, the hematite is probably in part hypogene. Only five samples contained zeolites; three from the western end of the Gooseberry fault, and two from the northwest quarter of section 36. The zeolites appear to be stilbite and heulandite.

SMECTITE-QUARTZ ASSEMBLAGE

Diagnostic minerals of this assemblage are smectite and quartz; illite and/or mixed-layer clays may also be present. The smectite-quartz assemblage is found in narrow, discontinuous zones along the Gooseberry fault, the subparallel structure just north of the Gooseberry fault, and the Red Top structure east (Plate II); it has not been observed underground.

Smectite-quartz assemblage rocks are off-white to pale yellow; relict plagioclase phenocrysts cannot be distinguished from the groundmass in hand sample. The rock crumbles readily and tends to erode away rather than to crop out. Most exposures of the smectite-quartz assemblage are in small prospect pits and trenches.

Smectite is the most common constituent, followed by

quartz. Illite is generally present in minor amounts and mixed-layer clays are not common. Metastable, partially altered plagioclase phenocrysts can be identified microscopically; their occurrence is extremely rare.

ILLITE-QUARTZ ASSEMBLAGE

The illite-quartz assemblage is characterized by the presence of illite and quartz. The rocks of this assemblage are off-white to pale yellow and look similar to the smectite-quartz assemblage in outcrop. However, the illite-quartz assemblage has a greasy feel when rubbed between the fingers, whereas the smectite-quartz assemblage does not.

This assemblage was mapped in only one locality near the Gooseberry vein, one locality near the parallel structure just north of the Gooseberry fault, and filling a fracture at the 200 level (Plates II and III). It may be present elsewhere on the property, but erodes too easily to remain exposed.

DICKITE-SILICA ASSEMBLAGE

The dickite-silica assemblage is characterized by the presence of dickite (see Appendix C for identification details). The silica occurs as quartz, quartz and opal,

or cristobalite. In outcrop, rocks of this assemblage range from off-white to yellow-orange. They do not crumble with finger pressure and have a low specific gravity. Relict plagioclase phenocrysts commonly stand out as white, blocky patches against a slightly darker groundmass. In thin section, relict plagioclase phenocrysts composed entirely of dickite can be observed. No other relict textures persist.

This assemblage occurs in the large altered area south of the Gooseberry vein (Fig. 3, Plate II). Dickite and quartz are the dominant minerals present along the Red Top structure east. To the west, rocks of the dickite-silica assemblage contain minor alunite. Here the silica occurs as quartz, quartz and opal, or cristobalite (Appendix C).

SILICIFICATION

Silicified rocks, as the term is used herein, refers to rocks that contain greater than 80 percent quartz. Wall-rock silicification, not common at the Gooseberry mine, occurs in a small area over the western end of the Gooseberry fault and near the eastern limit of P1 alteration (Plate II). The limited occurrence of silicified rock suggests that silicification was minor during wall-rock alteration; therefore, it will not be addressed further in this paper.

HORIZONTAL ZONATION OF HYDROTHERMAL ALTERATION ASSEMBLAGES

Adjacent to the Gooseberry Vein

In a few localities along the Gooseberry fault zone the illite-quartz assemblage and/or the smectite-quartz assemblage occur (Plate II). Where both assemblages are present, rocks of the illite-quartz assemblage are at the center; they grade outward to rocks of the smectite-quartz assemblage, which in turn grade outward to propylitized rocks (Plate II).

Adjacent to the Red Top Structures

Along the Red Top structures rocks of the dickite-silica assemblage grade outward to either the smectite-quartz assemblage or the propylitic assemblage (Plate II). Note that exposure is generally very limited near the dickite-silica occurrences. It is entirely probable that the dickite-silica assemblage is completely enveloped by the smectite-quartz assemblage, but that the friable nature of the rocks of the smectite-quartz assemblage prevents their exposure in outcrop.

VERTICAL ZONATION OF HYDROTHERMAL ALTERATION ASSEMBLAGES

The only alteration assemblage exposed underground along the vein is the propylitic assemblage; only type P1 occurs (Plate III). At the present-day surface the smectite-quartz assemblage and the illite-quartz assemblage both occur. Unfortunately, lack of access to, and exposure along, the Gooseberry vein from the 500 level to the surface prevent direct observation of the deepest occurrence of these two assemblages.

Vertical zonation of the individual minerals of the propylitic assemblage was discussed above (see Propylitic Assemblage section).

SUPERGENE ALTERATION

Clay minerals form by both hypogene and supergene processes. It is difficult to distinguish between hypogene and supergene products; however, some differences do occur. Dickite is believed to be largely hypogene in origin (Ross and Kerr, 1930). Montmorillonite is not as characteristic of supergene alteration as is kaolinite (Meyer and Hemley, 1967). Supergene products are generally zoned vertically, whereas hypogene products are commonly zoned horizontally as well as vertically.

Most of the clay minerals present at the Gooseberry

mine are believed by this author to be hydrothermal in origin, with a weak supergene overprint at the surface. The horizontal zoning pattern of the alteration assemblages suggests a hypogene origin. If supergene processes alone were responsible for the clay mineralogy it would be difficult to explain the horizontal zonation of the illite-quartz and the smectite-quartz assemblages; rather, a vertical zonation of some sort would be expected. Additionally, the abundance of smectite and the lack of kaolinite suggest a hydrothermal origin.

Supergene processes at the Gooseberry mine are undoubtedly responsible for the oxidation of pyrite and the presence of jarosite, goethite, and hematite at and near the surface. However, these processes did not cause the hydrothermal alteration assemblages to form.

VARIATIONS IN THE ATTITUDE, THICKNESS, AND METAL CONTENT
OF THE GOOSEBERRY VEIN

INTRODUCTION

The vein contouring technique was utilized to identify variations in strike and dip of the Gooseberry vein. This technique was found by Connolly (1936) to be useful in predicting the location of structurally-controlled ore shoots. Briefly, a reference plane that approximates the strike and dip of the vein is chosen and placed arbitrarily in the footwall. The distance from this reference plane to known points along the vein is calculated, plotted, and contoured, thus creating a longitudinal projection of the vein that shows structure contours.

Vein thickness, assay, and metal-ratio overlays can be prepared from the same data points. By overlaying the vein thickness longitudinal projection on the structure contour longitudinal projection, any correlation between vein thickness and attitude will generally be apparent. Likewise, any correlation between ore shoot location and vein attitude, or between metal-ratio variation and vein attitude, can be identified by overlaying the appropriate longitudinal projection on the structure contour longitudinal projection. This method has been utilized

successfully as an exploration tool in recent years (e.g., Buchanan, 1980; Clifton et al., 1980).

Appendix D describes how the structure contour longitudinal projection and accompanying overlays were constructed for this study and discusses the source of the assay data from which Plates VIII and IX were constructed.

LONGITUDINAL PROJECTION OF THE RECONSTRUCTED GOOSEBERRY VEIN SHOWING STRUCTURE CONTOURS

The longitudinal projection of the reconstructed Gooseberry vein showing structure contours (Plate V) reveals variations in the attitude of the vein. A composite plan map and several cross sections of the reconstructed Gooseberry vein (Plate VI) have been constructed from the structure contour longitudinal projection and the vein thickness longitudinal projection to aid in visualizing the form of the vein.

The reconstructed vein exhibits three distinctly different strikes (Plate VI). The westernmost section strikes approximately $N72^{\circ}W$. The strike gradually approaches $N88^{\circ}W$ in the central part then changes abruptly to approximately $N50^{\circ}W$ in the eastern part.

The dip also varies significantly (Plate VI). The central part of the vein dips steeply to the south. The eastern section between the 800 and 1000 levels flattens

to approximately 55°S . The westernmost segment between the 800 and 1000 levels exhibits a reversal in dip direction; the dip here is 75°N .

LONGITUDINAL PROJECTION OF THE RECONSTRUCTED GOOSEBERRY VEIN SHOWING VEIN THICKNESS CONTOURS

The Gooseberry vein ranges from one to twenty feet in thickness; the average width is seven feet. A comparison of the structure contour longitudinal projection (Plate V) with the vein thickness longitudinal projection (Plate VII) shows that the thickest part of the vein corresponds with the westerly limb of the large curve in the vein. A left-lateral strike-slip component to the movement along the fault prior to, and/or during, vein emplacement could have created a dilation zone on the west limb of this curve (Fig. 5A).

The western and central sections of the vein tend to thicken with depth, whereas the eastern segment does not (Plate VII). The western section exhibits a reversal in dip direction (Plate VI). Normal dip-slip movement would create a dilation zone below the point of dip reversal and a constriction above that point (Fig. 5B), thus explaining the tendency of this segment of the vein to thicken with depth. In the central part of the vein, the dip remains relatively constant (Plate VI). Here, dip-slip motion

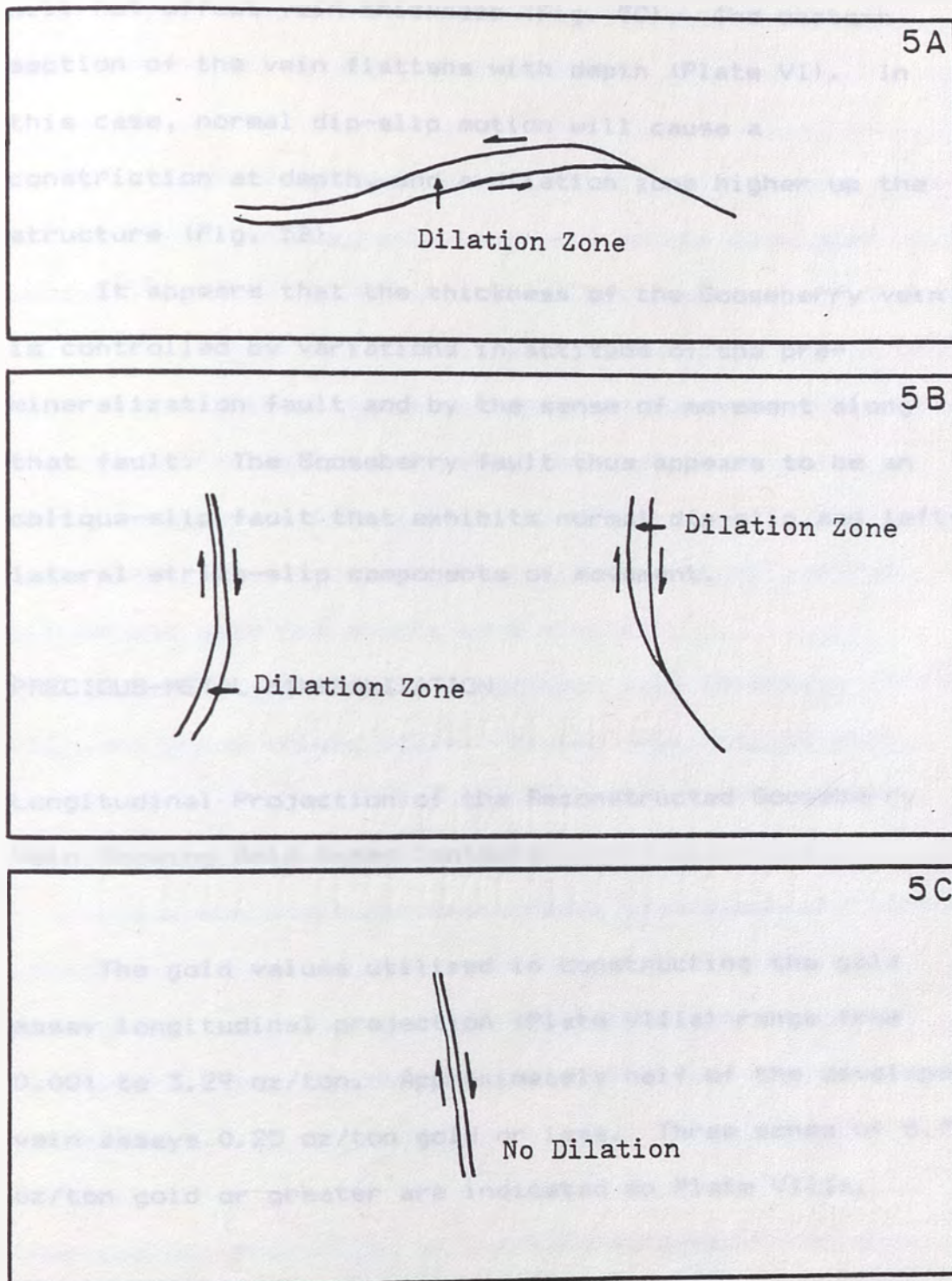


Fig. 5. Diagrammatic representation of left-lateral strike-slip (A) and dip-slip (B, C) movement along the Gooseberry fault. A. Plan view. B. Change in dip. Cross section view. C. No change in dip. Cross section view.

will not affect vein thickness (Fig. 5C). The eastern section of the vein flattens with depth (Plate VI). In this case, normal dip-slip motion will cause a constriction at depth, and a dilation zone higher up the structure (Fig. 5B).

It appears that the thickness of the Gooseberry vein is controlled by variations in attitude of the pre-mineralization fault and by the sense of movement along that fault. The Gooseberry fault thus appears to be an oblique-slip fault that exhibits normal dip-slip and left-lateral strike-slip components of movement.

PRECIOUS-METAL MINERALIZATION

Longitudinal Projection of the Reconstructed Gooseberry Vein Showing Gold Assay Contours

The gold values utilized in constructing the gold assay longitudinal projection (Plate VIIIa) range from 0.001 to 3.29 oz/ton. Approximately half of the developed vein assays 0.25 oz/ton gold or less. Three zones of 0.75 oz/ton gold or greater are indicated on Plate VIIIa.

Longitudinal Projection of the Reconstructed Gooseberry
Vein Showing Silver Assay Contours

The contoured silver values (Plate VIIIb) range from 0.1 to 98 oz/ton; approximately half of the developed vein assays 10 oz/ton silver or less. Three zones of 20 oz/ton silver or greater are indicated on Plate VIIIb. Note that the zones of higher-grade silver correspond with the zones of higher-grade gold; likewise, zones of lower-grade silver correspond with zones of lower-grade gold. Apparently, the structural controls that localized the silver and gold ore shoots were similar.

No correlation is noted between vein thickness (Plate VII) and grade (Plate VIII). Moving from west to east, the three high-grade ore shoots correspond with vein thicknesses of five, two, and ten feet, respectively.

The westernmost and easternmost high-grade ore shoots coincide with abrupt changes in dip of the vein. Apparently, sudden changes in the dip of the structure have contributed in creating favorable sites for ore deposition.

Longitudinal Projection of the Reconstructed Gooseberry
Vein Showing Silver-to-Gold Ratio Contours

Silver-to-gold ratios range from 12 to 367. The

ratio appears to be completely independent of structural trends and vein thickness, but does increase markedly with depth (Plate IXa). This is common in other precious-metal, volcanic-hosted, epithermal systems (Buchanan, 1981). Examples include Aurora, Nevada (Osborne, 1985) and Tonopah, Nevada (Nolan, 1935). Goodell and Petersen (1974) report both vertical and lateral variations in Pb/Cu, Ag/Pb, and Ag/Cu ratios from the Julcani district, Peru; they did not use the Ag/Au ratio.

Buchanan (1981) invokes boiling, and its accompanying chemical changes, including loss of H_2O , CO_2 , and H_2S to the vapor phase, a rise in salinity and oxygen fugacity, and a slight cooling of the solution, as one viable explanation for this systematic variation in silver-to-gold ratios.

The shape of the contours resulting from metal-ratio studies has been related to the direction of movement of the mineralizing fluids (Goodell and Petersen, 1974; Petersen et al., 1977). The marked variation with depth of the Ag/Au ratios at the Gooseberry Mine indicates that the mineralizing fluids moved upward, rather than laterally.

Longitudinal Projection of the Reconstructed Gooseberry Vein Showing Equivalent-Silver-Foot Contours

Plate IXb is a combination of the gold, silver, and

thickness data. For each data point, gold assays were converted to their silver equivalent by multiplying by 51 (see Appendix D); their sum was multiplied by the vein thickness at that point. The results ranged from 1 to 935 oz-ft/ton; over two-thirds of the developed vein exhibits an equivalent-silver-foot number of greater than 100 oz-ft/ton (Plate IXb). Depending upon ground conditions, mining costs, and metals prices, an equivalent-silver-foot number of less than 50 oz-ft/ton is probably uneconomical to mine, whereas an equivalent-silver-foot number of greater than 100 oz-ft/ton is generally economical to mine.

Vein thickness affects the equivalent-silver-foot numbers the most; however, gold and silver grades are also reflected in the contour lines in Plate IXb. The western and eastern zones of higher numbers (Plate IXb) correspond with the western and eastern high-grade ore shoots discussed in the Longitudinal Projection of the Reconstructed Gooseberry Vein Showing Silver Assay Contours section, above; their location was probably controlled by abrupt changes in dip of the vein. The central zone of higher numbers coincides with the western limb of the major curve in the structure. Here silver and gold grades are moderate, but the vein is much thicker. The ore-shoot control in this case is a change in the strike of the fault combined with left-lateral strike-slip

motion along the fault (see Longitudinal Projection of the Gooseberry Vein Showing Vein Thickness Contours section, above).

The detailed stratigraphic column of the Gooseberry vein was obtained from the 1930-1931 section which was made in 1931 before the faulting. Although fluid-inclusion data cannot be correlated with the vein stages of this locality, they can be utilized to obtain an approximate time sequence of the faulting. The data indicate that the faulting was probably completed before the deposition of the uppermost layers of the vein. This is supported by the fact that the faulting is not observed in the uppermost layers of the vein. The faulting is also supported by the fact that the faulting is not observed in the uppermost layers of the vein. The faulting is also supported by the fact that the faulting is not observed in the uppermost layers of the vein.

DISCUSSION

The data indicate that the faulting was probably completed before the deposition of the uppermost layers of the vein. This is supported by the fact that the faulting is not observed in the uppermost layers of the vein. The faulting is also supported by the fact that the faulting is not observed in the uppermost layers of the vein. The faulting is also supported by the fact that the faulting is not observed in the uppermost layers of the vein.

FLUID-INCLUSION STUDIES

INTRODUCTION

A detailed paragenetic study of the Gooseberry vein was excluded from this project because the mine staff denied access to the stopes. Although fluid-inclusion data cannot be correlated with various stages of vein deposition, they can be utilized to obtain an approximation of conditions during vein deposition.

Vein samples that were mineralized with base- and precious-metal sulfides and sulfo-salts other than pyrite were chosen in order to maximize the chances of working with ore-stage material (L. Buchanan, oral communication, 1983). Of the eight samples obtained for fluid-inclusion study, only three contained noncracked, primary fluid inclusions. Plate IV shows the sample locations; sample preparation methods and the heating-freezing equipment used are described in Appendix E.

SAMPLE DESCRIPTIONS

Sample FI-6, collected in the stope above the 1004 cross cut (Plate IV), is composed of very fine-grained quartz after calcite. The inclusions chosen for heating are as large as 50 microns by 10 microns in size, are

relatively isolated from neighboring inclusions, and are interpreted as being primary (Table 2). Those with visible cracks were eliminated, as were all inclusions that showed evidence of necking down (Roedder, 1984). Planes of probable secondary inclusions were avoided. Neither daughter minerals nor liquid CO_2 were seen in any of the inclusions.

Sample FI-6 contains zones of very tiny inclusions that appear darker than the larger inclusions and that commonly parallel crystal faces. Unfortunately, many of these small inclusions could not be resolved using a 100 power oil immersion objective with a numerical aperture of 1.25. Of the inclusions that could be resolved, most appear to contain from one to fifteen volume percent vapor, a few appear to contain only vapor, and a few appear to contain only liquid. Individual inclusions are elongated perpendicular to growth bands in the crystals.

Sample FI-2, obtained from the 850 stope (Plate IV), consists of calcite with a minor amount of very fine-grained quartz after calcite. The quartz contains inclusions that are very similar to those described in FI-6, above. The calcite contains large, primary inclusions and numerous planes of probable secondary inclusions; no zones of small inclusions were observed in the calcite. All the inclusions from which homogenization temperature data were obtained for this sample were in calcite.

Table 2. Summary of Criteria for Primary Origin of Fluid Inclusions.

-
1. Based on occurrence in a single crystal, with or without evidence of direction of growth or growth zonation.
 - A. Occurrence as a single inclusion in an otherwise inclusion-free crystal.
 - B. Large size relative to that of the enclosing crystal, particularly several such inclusions.
 - C. Isolated occurrence, away from other inclusions, for a distance of approximately 5 times the diameter of the inclusion.
 - D. Occurrence as part of a random, three-dimensional distribution throughout the crystal.

 2. Based on occurrence in a single crystal showing evidence of growth zonation.
 - A. Occurrence in random three-dimensional distribution, with different concentrations in adjacent zones.
 - B. Occurrence as subparallel groups (outlining growth directions), particularly with different concentrations in adjacent zones.
 - C. Multiple occurrence in planar array(s) outlining a growth zone.
-

Modified from Roedder (1984).

Sample FI-4, collected from the 806 stope (Plate IV), is very similar in appearance to FI-2, but contains more abundant, very fine-grained quartz after calcite. As in FI-2, the quartz exhibits zones of tiny inclusions similar to those in FI-6, but the calcite does not.

The remaining five samples closely resemble FI-2. No uncracked primary inclusions were observed in any of these samples, in spite of preparing two polished plates for many of them.

These eight vein samples support Kleeberger's (undated) statement that calcite was deposited first and was followed by quartz deposition (see Vein Mineralogy section, above). In these samples, quartz replaced some of the calcite. It is unknown whether all of the quartz in the vein replaced calcite or whether some of the quartz is primary. Note that roughly 90 percent of the vein is composed of calcite.

BOILING VERSUS EFFERVESCENCE

Boiling involves the release of a low-density phase that is the same composition as the liquid, whereas effervescence involves the release of a low-density phase that is compositionally different from the liquid (Roedder, 1984). These two processes are actually end members of a continuum and can be difficult to distinguish (Roedder, 1984). Both processes should result in fluid-inclusion

evidence that two immiscible fluids coexisted; the most unequivocal evidence is the coexistence of liquid-dominated inclusions and vapor-dominated inclusions (Roedder, 1984).

Kamilli and Ohmoto (1977) discuss two types of boiling. The first type does not noticeably affect the rate of crystal growth or of crystal size; it is believed to result in inclusions with a low liquid/vapor ratio coexisting with inclusions with a high liquid/vapor ratio (Kamilli and Ohmoto, 1977). However, when minerals are rapidly precipitated by boiling fluids, crystals grow faster and are often very fine-grained; the resulting inclusions generally exhibit random liquid/vapor ratios (Kamilli and Ohmoto, 1977).

Rapid precipitation of vein material by boiling fluids has been extensively discussed in the literature (e.g., Kamilli and Ohmoto, 1977; Buchanan, 1979; Sawkins et al., 1979; Fahley, 1981; Bruha, 1983; and Roedder, 1984). It has been cited as one cause of zones of very small inclusions similar to those that occur in the vein quartz at the Gooseberry mine (Kamilli and Ohmoto, 1977; Buchanan, 1979; Fahley, 1981; Bruha, 1983). Table 3 summarizes eight criteria that have been associated with rapid precipitation of vein material by boiling. Criterion number 4, variable homogenization temperatures of primary inclusions, is considered the most convincing proof of this type of boiling; unfortunately, the inclusions that texturally

Table 3. Summary of Evidence for Rapid Precipitation of Vein Material by Boiling at the Gooseberry Mine.

	Applies to calcite?	Applies to quartz?
1. Mineralization controlled by elevation? (1, 2, 3)	Yes	Yes
2. Fine-grained ore and gangue? (1, 3)	No	Yes
3. Highly variable liquid to vapor ratios in primary inclusions? (1, 2, 3, 4)	No	Probable
4. Variable homogenization temperatures of primary inclusions? (1, 2, 3)	No	Inclusions too small to measure
5. Tiny inclusions, irregular in shape, with the long axis perpendicular to crystal growth bands? (2)	No	Yes
6. Fluid inclusions aligned in radiating bands? (2, 3)	No	Yes
7. Highly shredded gangue? (2, 3)	No	Common
8. Widely variable salinity? (2, 3, 5)	Not determined	

(1) Kamilli and Ohmoto (1977)

(2) Buchanan (1979)

(3) Fahley (1981)

(4) See text, Sample Description section

(5) See text, Salinity Estimate section

appear to indicate boiling are too small to provide homogenization temperature data.

Of the eight criteria listed in Table 3, only the first applies to calcite from the Gooseberry vein; therefore, the calcite was evidently deposited slowly by non-boiling fluids. In addition, the primary fluid inclusions contained in the calcite all have approximately the same liquid/vapor ratio. If gases, such as CO_2 , were effervescing, it is expected that some gas-rich inclusions would be evident (Roedder, 1984). Therefore, it appears that the effervescence of gas from the hydrothermal fluids did not play a major role during calcite deposition.

Four of the eight criteria associated with rapid precipitation of vein material by boiling (Table 3) always apply to the vein quartz (numbers 1, 2, 5, and 6), another commonly applies (number 7), and still another probably applies (number 3). The size of the inclusions precludes direct observation of two of the criteria, numbers 4 and 8. The available data, then, indicate that rapid precipitation of vein material by boiling probably occurred sporadically during quartz deposition; however, the evidence is not sufficient to prove that boiling actually occurred.

HOMOGENIZATION TEMPERATURES

The homogenization temperature ranges and medians are listed in Table 4. A histogram of the homogenization temperatures (Fig. 6) exhibits a bell-shaped distribution with the exception of the 225 to 230°C range.

The overabundance of temperatures in the 225 to 230°C range is believed to be due to undetected cracked or necked-down inclusions. Hence, homogenization temperatures are best represented by the 240 to 245°C range. Because these temperatures are not believed to be related to boiling (see preceding section), a temperature correction as a result of pressure is required. Under the estimated conditions of deposition, this correction is negligible (Potter, 1977).

Recall that the fluid inclusion data presented here are only preliminary. A more complete fluid inclusion study, including a vein paragenesis study, could result in differing results.

SALINITY ESTIMATE

Appreciable time was spent attempting to freeze primary inclusions in sample FI-6 to estimate the salinity of the trapped fluid. No visible changes occurred in the inclusions for the temperature range +25 to -50°C. This

Table 4. Homogenization Temperature Range and Median.

Sample no.	Homogenization temp. range degrees C	No. of inclusions measured	Median temp. degrees C
FI-2	226 - 256	11	242
FI-4	225 - 251	8	239
FI-6	222 - 268	10	239
composite	222 - 268	29	240

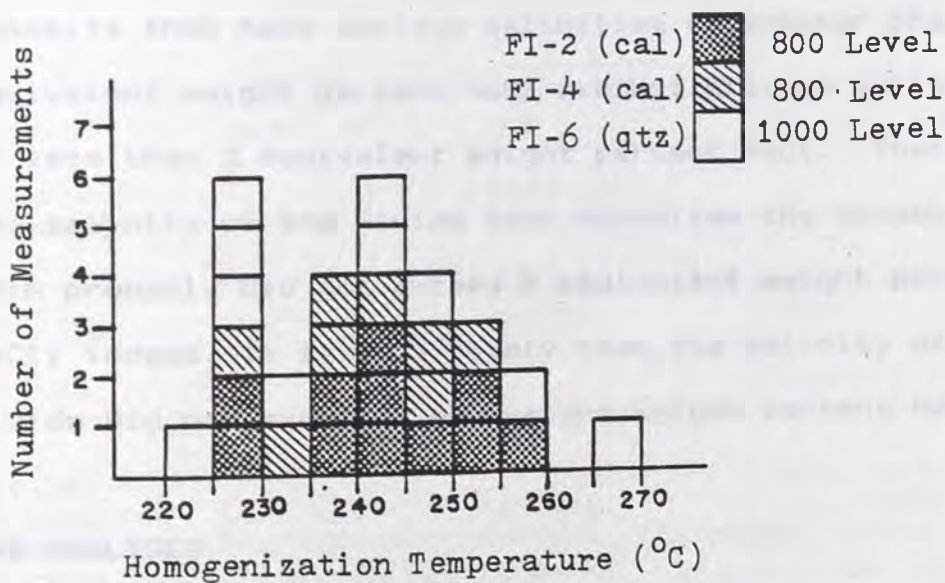


Fig. 6. Composite histogram of homogenization temperatures.

could be due to a low salinity content of the fluids, because the refractive index of a low-salinity fluid is so similar to that of its ice, that it is often very difficult to distinguish between them (D. Bruha, oral communication, 1984).

Epithermal deposits as a group are characterized by low-salinity fluids, commonly less than five equivalent weight percent NaCl (Roedder, 1984). Table 5 lists the salinity ranges resulting from fluid inclusion studies of twelve epithermal vein deposits that are similar to the Gooseberry mine. The maximum observed salinity from five of the deposits is less than 2 equivalent weight percent NaCl; the maximum from three additional deposits ranges from 2.1 to 2.6 equivalent weight percent NaCl. The three deposits that have maximum salinities of greater than 4 equivalent weight percent NaCl exhibit minimum salinities of less than 2 equivalent weight percent NaCl. Therefore, the salinity of the fluids that deposited the Gooseberry vein probably did not exceed 5 equivalent weight percent NaCl; indeed, it is very likely that the salinity of these fluids did not exceed 2 equivalent weight percent NaCl.

GAS ANALYSES

Seven separate vein samples were analyzed by Exploration Research Laboratories in Salt Lake City, Utah,

Table 5. Salinity Ranges Resulting from Fluid-Inclusion Studies of Various Epithermal, Volcanic-Hosted, Precious-Metal, Low-Sulfide, Vein Deposits.

District	Salinity range Eq. wt. % NaCl	Mineralogy of vein	References
Bodie, California	0.3	Au-Ag-qtz- ad-cal	O'Neil et al., 1973
Eureka, Colorado	0.3-2.2	Au-tell-qtz	Casadevall and Ohmoto, 1977 (1)
Aurora, Nevada	0.2-1.7	Au-qtz-ad	Nash, 1972
Manhattan, Nevada	0.3-1.9	Au-qtz-ad	Nash, 1972
National, Nevada	1.3-2.1	Ag-Au-qtz	Vikre, 1985
Round Mtn., Nevada	0.2-1.4	Au-qtz-ad	Nash, 1972
Tenmile, Nevada	0.4-7.3	Au-qtz-ad	Nash, 1972
Tonopah, Nevada	0.6-2.6	Ag-Au-qtz- ad	Fahley, 1981
Guanajuato, Mexico	<1	Ag-Au-qtz- ad-cal	Buchanan, 1981
Tayoltita, Mexico	1.9-9.7	Ag-Au-qtz- ad-cal	Smith et al., 1982
Colqui, Peru	0.2-10.8	Ag-Au-qtz	Kamilli and Ohmoto, 1977 (2)
Baguio, Philippines	0.4-4.6	Au-qtz	Sawkins et al., 1979

Abbreviations: Au = gold; Ag = silver; qtz = quartz; ad = adularia; cal = calcite, tell = tellurides.

(1) This vein mineralogy and salinity range are only from Period IV, the gold-telluride ore shoots.

(2) This vein mineralogy and salinity range are only from Stage II, the Ag-Au ore shoots.

for gas content of fluid inclusions; the technique used is semi-quantitative rather than quantitative. Appendix F describes the analytical equipment and sample preparation methods utilized. The primary reason for obtaining gas analysis data from the Gooseberry vein was to determine whether CO_2 is present in the fluid inclusions. Because the paragenetic relationship of the samples is unknown, it cannot be determined if the gas content changes in a systematic fashion, either spatially or paragenetically.

Samples 1, 2, 3, 4, 5, 6, and 8 correspond to FI-1, FI-2, FI-3, FI-4, FI-5, FI-6, and FI-8, respectively; see Plate IV for locations. Sample 4 is quartz + calcite as it occurs in FI-4; sample 10 is only quartz from FI-4. Samples 6 and 9 are duplicate samples of quartz from FI-6.

Table 6 lists the reported micrograms of gas evolved per gram of sample, rounded off to three significant figures, and the relative percentage of each gas. The most abundant gas measured is CO_2 (86.4 to 99.2 percent of the analyzed gases); CS_2 occurs in minor amounts (0.35 to 9.8 percent); COS , H_2S , C_2H_6 , and C_3H_8 occur in minute to minor amounts; and the amount of SO_2 and CH_4 is negligible.

Samples 6 and 9, replicates, show results that are reasonably close, indicating that the technique is reproducible in a semi-quantitative manner. Sample 4, quartz and calcite, and sample 10, quartz, also show gas analysis results that are close, indicating that the

Table 6. Gas Analysis Data from Fluid-Inclusion Samples from the Gooseberry Vein¹

Gas analysis sample no.	Fluid inclusion sample ₂ no.	CS ₂	SO ₂	COS	CO ₂	H ₂ S	CH ₄	C ₂ H ₆	C ₃ H ₈	Total
1	FI-1	250 (2.9) ³	3.6 (0.04)	20.4 (0.24)	7560 (88.4)	169 (2.0)	23 (0.27)	231 (2.7)	293 (3.4)	8550 (100)
2	FI-2	47 (0.69)	1.4 (0.02)	10.7 (0.16)	6580 (97.5)	ND ⁴	3 (0.04)	51 (0.76)	60 (0.89)	6750 (100)
3	FI-3	353 (4.2)	12.1 (0.15)	15.0 (0.18)	7810 (93.8)	ND	6 (0.07)	81 (0.97)	54 (0.65)	8330 (100)
4 ⁵	FI-4	389 (7.1)	9.4 (0.17)	67.2 (1.2)	4920 (89.6)	ND	3 (0.05)	35 (0.64)	62 (1.1)	5490 (100)
10 ⁵	FI-4	478 (9.8)	16.9 (0.35)	76.6 (1.6)	4210 (86.4)	ND	4 (0.08)	45 (0.93)	40 (0.82)	4870 (100)
5	FI-5	43 (0.35)	ND	6.1 (0.05)	12000 (99.2)	ND	4 (0.03)	58 (0.48)	33 (0.27)	12100 (100)
6 ⁶	FI-6	500 (9.8)	ND	42.8 (0.84)	4490 (88.0)	ND	1 (0.02)	25 (0.49)	39 (0.76)	5100 (100)
9 ⁶	FI-6	318 (8.0)	2.5 (0.06)	38.3 (0.97)	3530 (89.1)	ND	3 (0.08)	30 (0.76)	40 (1.0)	3960 (100)
8	FI-8	41 (0.89)	ND	6.2 (0.14)	4490 (97.6)	ND	2 (0.04)	27 (0.59)	29 (0.63)	4600 (100)
average										6640
median										5490

¹Analyses reported in micrograms of gas evolved per gram of sample, but see discussion in text.

²Sample locations are given on Plate IV. ³Numbers in parentheses are relative percentages of the given gas species. ⁴ND = none detected. ⁵Sample 4 is quartz and calcite from FI-4, whereas sample 10 is quartz only. ⁶Samples 6 and 9 are duplicate samples.

abundant planes of secondary inclusions observed in the calcite contain gases similar to those in the primary inclusions.

Bruha (1983) concluded that "the MIDECO analyses are incorrect in magnitude" for samples from Mina Teresita, Peru, that he submitted to MIDECO (now Exploration Research Laboratories). A similar evaluation can be performed for these samples. The average total gas measured is approximately 6000 ppm (Table 6). Therefore, roughly 0.6% of the sample, by weight, is gas.

The actual water content cannot be determined by Exploration Research Laboratories' analytical equipment, but it can be extrapolated. Fluid inclusions from the Finlandia vein, Colqui district, Peru, contain from 94 to 99 weight percent H_2O and from 6 to 1 weight percent all other gases (Kamilli and Ohmoto, 1977); those from the Sunnyside mine, Eureka district, Colorado, contain from 95 to 99.9 weight percent H_2O and from 5 to 0.1 weight percent all other gases (Casadevall and Ohmoto, 1977); those from vein gold deposits, Baguio district, Philippines, contain from 97.7 to 99.98 weight percent H_2O and from 2.3 to 0.02 weight percent all other gases (Sawkins et al., 1979; the above values were calculated from reported mole fraction data). Gas concentrations ranging from 0.05 to 1 weight percent have been reported from several geothermal fields (Henley et al., 1984). Therefore, it can be assumed that the fluid inclusions obtained from the Gooseberry vein are

composed of at least 94 weight percent H_2O ; a minimum estimate of 98 weight percent H_2O would be more realistic.

If two percent of the total trapped fluid is gas, then two percent of the total trapped fluid equals the gas content of the sample, or 0.6 weight percent of the sample.

$$(0.02)(\text{total trapped fluid}) = 0.6 \text{ wt } \%$$

$$\text{total trapped fluid} = 0.6 \text{ wt } \% / 0.02$$

$$= 30 \text{ wt } \%$$

Solving the above equation yields a total trapped fluid content of 30 weight percent of the sample. If the same calculation is performed assuming the inclusions are 94% H_2O , a figure that is probably too low, the total trapped fluid content would be 10 weight percent of the sample.

Optical examination of the fluid inclusion plates clearly shows that the fluid inclusions account for less than two volume percent of the vein; this is much lower than a weight percent of from 10 to 30. It appears, then, that the Exploration Research Laboratories' analyses of specimens from the Gooseberry vein are incorrect in magnitude.

The gas analysis data are, however, helpful in determining the relative abundance of total carbon to total sulfur, and the relative oxidation state of the fluids (C. Clifton, written communication, 1984). Appendix G shows how to calculate these ratios, Table 7 lists the results, and Figure 7 is a log-log plot of total carbon/total sulfur

Table 7. Weight Ratios of Analyzed Volatiles.

Gas analysis sample no.	Fluid inclusion sample no.	Total C/ total S	Total ox. C+S/ total red. C+S
1	FI-1 (cal)	7.1	2.5
2	FI-2 (cal)	45.1	13.0
3	FI-3 (cal)	8.1	4.6
4	FI-4 (cal + qtz)	4.5	3.0
10	FI-4 (qtz)	3.2	2.2
5	FI-5 (cal)	92.7	27.5
6	FI-6 (qtz)	3.4	2.3
9	FI-6 (qtz)	4.1	2.6
8	FI-8 (cal)	3.2	2.21

Fluid inclusion sample locations are shown on Plate IV.

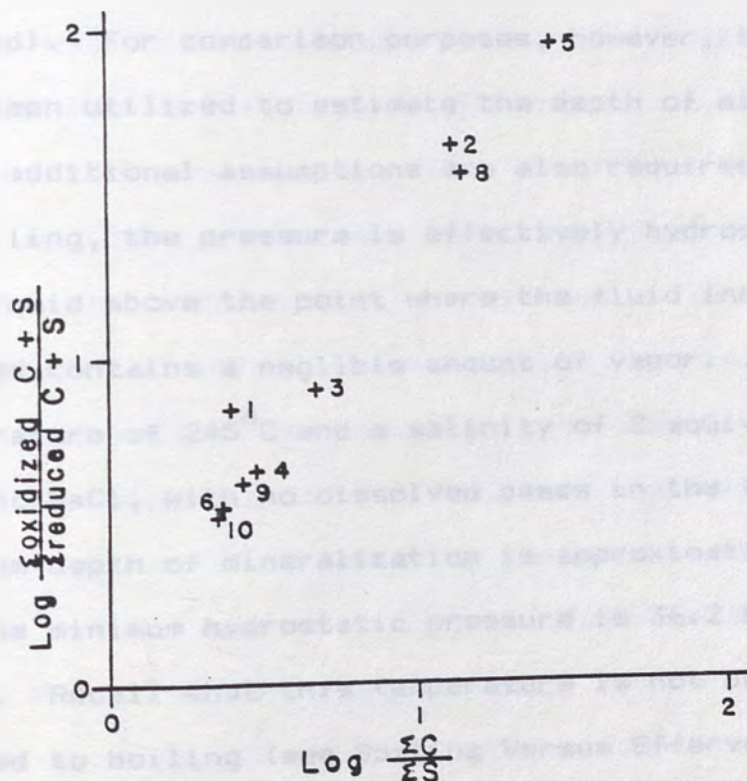


Fig. 7. Total C/total S - total oxidized (C + S)/total reduced (C + S) of analyzed volatiles.

versus total oxidized carbon plus sulfur/total reduced carbon plus sulfur. The fluids from these samples contain relatively more carbon than sulfur and relatively more oxidized carbon and sulfur than reduced carbon and sulfur.

DEPTH OF MINERALIZATION

Due to the presence of CO_2 in fluid inclusions contained in the Gooseberry vein, the data of Haas (1971) yield an estimate of the depth of mineralization that is too shallow (Takenouchi and Kennedy, 1965; Kamilli and Ohmoto, 1977; Holland and Malinin, 1979; Bodnar and Kuehn, undated). For comparison purposes, however, these data have been utilized to estimate the depth of mineralization. Three additional assumptions are also required: the fluid is boiling, the pressure is effectively hydrostatic, and the liquid above the point where the fluid inclusion was trapped contains a negligible amount of vapor. At a temperature of 245°C and a salinity of 2 equivalent weight percent NaCl, with no dissolved gases in the fluid, the minimum depth of mineralization is approximately 1346 feet and the minimum hydrostatic pressure is 36.2 bars (Haas, 1971). Recall that this temperature is not believed to be related to boiling (see Boiling Versus Effervescence section, above); therefore, the estimated depth is too shallow and the estimated pressure is too low.

Mineralization at the Gooseberry mine is dated at 10.3 +/- 0.3 m. y. (see Age of Mineralization section, above). The Coal Valley Formation has been dated at 11.5 to 12.6 m. y. (Silberman and McKee, 1972; recalculated using present constants, Dalrymple, 1979); the Mustang Andesite, at 9.1 to 9.2 m. y. (Morton et al., 1977). Therefore, the Coal Valley Formation was deposited approximately one million years prior to, and the Mustang Andesite was deposited approximately one million years after, mineralization.

Ore-grade vein material is known to extend at least to the 1150 level; its lower limit has not yet been determined (R. Karlson, oral communication, 1985). A reasonable minimum estimate of the lower limit of mineralization would therefore be 1200 feet below the present surface. The 1300 level of the mine exposes a flow breccia of the Kate Peak Formation; this breccia may be a basal flow of the Kate Peak Formation (D. Hudson, oral communication, 1984). Assuming that this is the base of the Kate Peak Formation and that the Kate Peak Formation attained its maximum estimated thickness of 1500 feet here, approximately 200 feet of the Kate Peak Formation has subsequently been eroded. If the estimated maximum thickness of the Coal Valley Formation, 500 feet, has also been eroded from the present surface, an estimated minimum depth of the lower limit of mineralization would be 1900 feet below the paleosurface. The lower limit of mineralization can be no

shallower than 1150 feet below the paleosurface because mineralization is known to persist to 1150 feet below the present surface.

Based on the stratigraphic reconstruction, the depth of the lower limit of mineralization lies between 1150 and 1900 feet below the paleosurface. The minimum depth of mineralization below the paleosurface, using the data of Haas (1971), is 1346 feet. Therefore, the true depth of mineralization is probably between 1350 and 1900 feet below the paleosurface.

- 1. The fluid included in the weight percent of water, H₂O, was 5.00 percent, based on the relative gas proportions from the gas analysis and correct
- 2. The fluid is composed solely of H₂O and the analyzed gases.

Simple calculations are given in Appendix B; the results are listed in Table 3. The range of weight percent of CO₂, assuming the relative percent H₂O, was 0.51 and 0.70, respectively; assuming an weight percent H₂O, 0.81 and 0.90, respectively; assuming the weight percent H₂O, 0.21 and 0.18, respectively.

The amount of CO₂ in solution is governed by the pressure (see depth), the temperature, and the salinity of the fluid, utilizing the estimated weight of

Table 8. CHEMICAL PARAMETERS DURING ORE DEPOSITION

PARAMETERS AT DEPTH

Estimated Carbon Dioxide Content

Exploration Research Laboratories is not equipped to analyze for water content in fluid inclusions; therefore, an accurate measurement of CO_2 content is not possible. However, an attempt was made to calculate the mole percent of CO_2 based upon the following assumptions:

1. the fluid inclusion is 98 weight percent, or more, H_2O (see Gas Analysis section, above)
2. the relative gas proportions from the gas analyses are correct
3. the fluid is composed solely of H_2O and the analyzed gases.

Sample calculations are given in Appendix G; the results are listed in Table 8. The largest and smallest mole percents of CO_2 , assuming 98 weight percent H_2O , are 0.83 and 0.70, respectively; assuming 99 weight percent H_2O , 0.41 and 0.35, respectively; assuming 99.5 weight percent H_2O , 0.21 and 0.18, respectively.

The amount of CO_2 in solution is governed by the pressure (the depth), the temperature, and the salinity of the fluids. Utilizing the estimated depth of

Table 8. Estimated Mole Percent of Carbon Dioxide.

	Gas analysis sample no. 5	Gas analysis sample no. 10
Relative wt. % CO ₂ if:		
gases analyzed = 100%	99.2%	86.4%
" " = 2%	2.0%	1.7%
" " = 1%	0.99%	0.86%
" " = 0.5%	0.50%	0.43%
Mole % CO ₂ if:		
gases analyzed = 2%	0.83	0.70
" " = 1%	0.41	0.35
" " = 0.5%	0.21	0.18

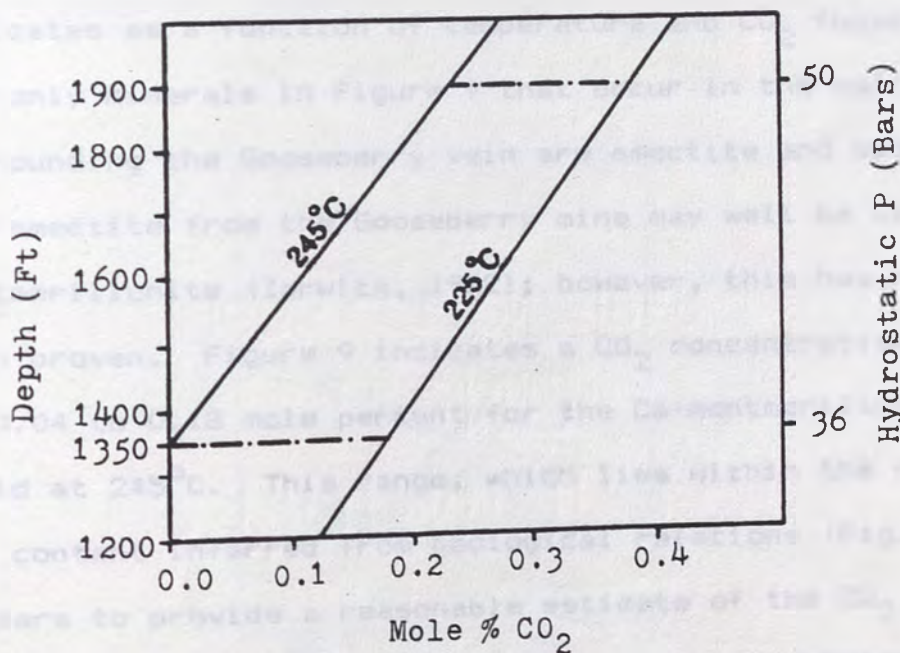


Fig. 8. Depth - carbon dioxide content at a salinity of 2 eq. wt. % NaCl.

mineralization range, 1350 to 1900 feet, the possible temperature of mineralization range, 225 to 245°C, and a salinity of 2 equivalent weight percent NaCl, Figure 8 can be constructed. The data of Haas (1971; 1976) and the Henry's Law coefficient for CO₂ in solution (Ellis and Golding, 1963) are also necessary.

At a depth of 1900 feet, the mole percent CO₂ in solution at 225°C is 0.38; at 245°C it is 0.23 (Fig. 8). This suggests that the estimate of 0.70 to 0.83 mole percent CO₂, given above, is at least twice as large as permissible, and that the estimate of 0.35 to 0.41 mole percent CO₂ is probably also too large.

Figure 9 shows the stability of some calcium-aluminum silicates as a function of temperature and CO₂ fugacity. The only minerals in Figure 9 that occur in the wall rocks surrounding the Gooseberry vein are smectite and epidote. The smectite from the Gooseberry mine may well be Ca-montmorillonite (Zerwick, 1982); however, this has not yet been proven. Figure 9 indicates a CO₂ concentration range of 0.04 to 0.18 mole percent for the Ca-montmorillonite field at 245°C. This range, which lies within the range of CO₂ content inferred from geological relations (Fig. 8), appears to provide a reasonable estimate of the CO₂ content of the mineralizing system at the Gooseberry mine.

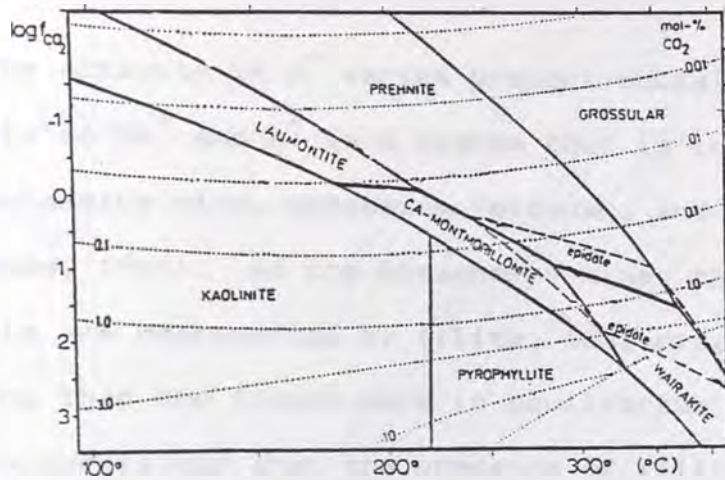


Fig. 9. The stability of Ca-aluminum silicates as a function of carbon dioxide and temperature, in equilibrium with chalcedony and calcite. Dotted lines are liquid-phase carbon dioxide isopleths in mole percents. The stability field of epidote is given for $X_{\text{pistacite}} = 0.22$. Stability boundaries above 320 degrees C are only schematic (modified from Giggenbach, 1984).

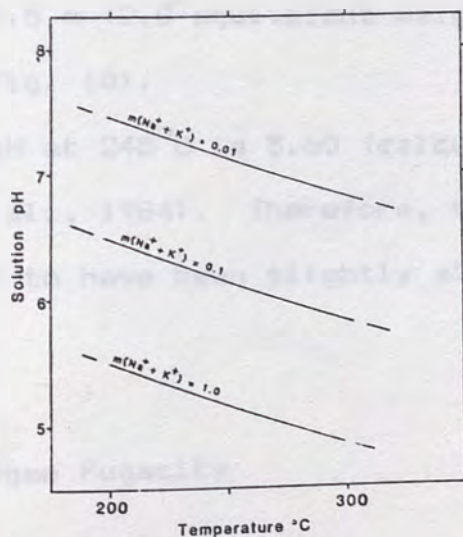


Fig. 10. Solution pH - temperature relations constrained by the Kspar-Kmica-quartz equilibrium at 3 salinities (modified from Henley et al., 1984).

Estimated pH

The activity of H^+ varies proportionately to the activity of Na^+ and K^+ in a system that is in equilibrium with potassium mica, potassium feldspar, and albite (Hemley and Jones, 1964). At the Gooseberry mine, these three minerals are represented by illite, adularia, and albite. Assuming that the fluids were in equilibrium with these three minerals and that the presence of illite rather than sericite did not appreciably affect the results, the pH can be estimated from Figure 10. A temperature of $245^{\circ}C$ and a salinity of not more than 0.5 m has been estimated for the mineralizing fluids (see Fluid-Inclusion Studies section, above). At $245^{\circ}C$, with a salinity of 0.1 m (0.58 equivalent weight percent NaCl), the pH is 6.16; at a salinity of 0.5 m (2.8 equivalent weight percent NaCl), the pH is 5.53 (Fig. 10).

Neutral pH at $245^{\circ}C$ is 5.60 (calculated from data given by Henley et al., 1984). Therefore, the mineralizing fluids appear to have been slightly alkaline to slightly acidic.

Estimated Oxygen Fugacity

A probable fO_2 range can be estimated from mineral stability relationships. Figure 11 shows the $\log fO_2$

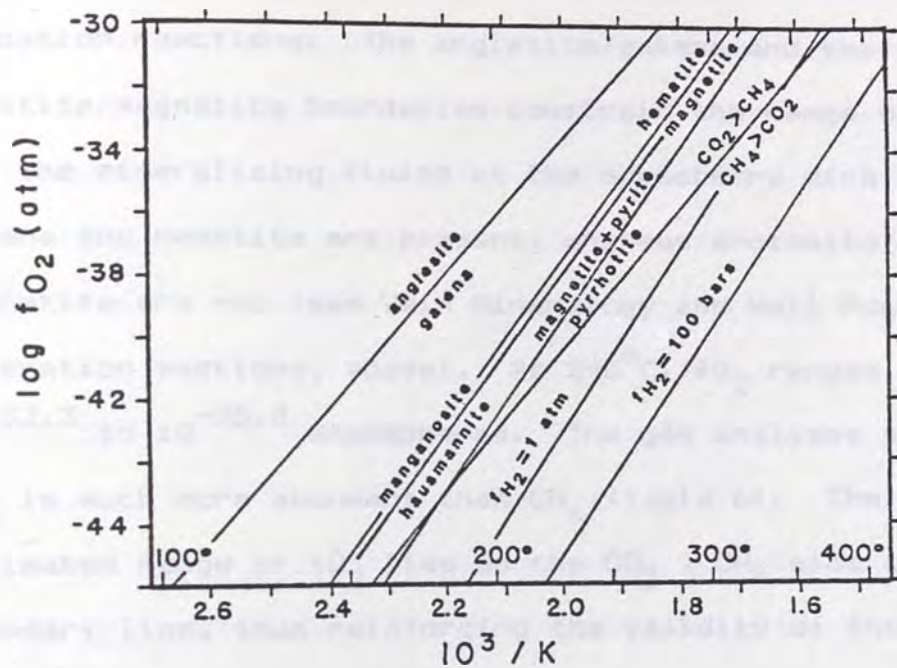


Fig. 11. Log oxygen fugacity - $1/T$ diagram showing typical oxidation reactions among minerals. The figures inside the lower margin are degrees C (after Henley et al., 1984).

versus the reciprocal of temperature for several typical oxidation reactions. The anglesite/galena and the hematite/magnetite boundaries constrain the range of f_{O_2} for the mineralizing fluids at the Gooseberry mine because galena and hematite are present, whereas anglesite and magnetite are not (see Vein Mineralogy and Wall Rock Alteration sections, above). At 245°C, f_{O_2} ranges from $10^{-32.3}$ to $10^{-35.8}$ atmospheres. The gas analyses show that CO_2 is much more abundant than CH_4 (Table 6). The estimated range of f_{O_2} lies on the $CO_2 > CH_4$ side of this boundary line, thus reinforcing the validity of the f_{O_2} estimate.

At Guanajuato, Mexico, f_{O_2} was estimated to be between $10^{-36.5}$ and $10^{-45.2}$ (Buchanan, 1979); at Tonopah, the O_2 fugacity was estimated to be between 10^{-32} and 10^{-34} (Fahley, 1981). Neither states whether the fugacity is in bars or atmospheres; however, since 0.986923 bars equals 1 atmosphere, the difference is slight.

Estimated Total Sulfur

The total sulfur content of mineralizing fluids can be determined by quantitative gas analyses (e.g., Buchanan, 1979); this technique was not done for this study.

The total sulfur content at Guanajuato is $10^{-2.5}$ moles (Buchanan, 1979); at Tonopah, the total sulfur content was

assumed to be 10^{-2} moles (Fahley, 1981). Based on the similarity of the altered wall rocks and vein mineralogy at Guanajuato, Tonopah, and the Gooseberry mine, it is not unreasonable to assume a total sulfur content of the mineralizing fluids at the Gooseberry mine of approximately 10^{-2} to $10^{-2.5}$ moles.

PARAMETERS AT THE SURFACE

The geologic literature documents the study of active hot spring systems and their resulting alteration suites, and discusses the convective hydrologic system underlying such hot springs (e.g., Schoen et al., 1974; Ellis, 1979; White, 1981; Henley and Ellis, 1983). One classic example is Steamboat Springs, Nevada (Schoen et al., 1974; Figure 1). The altered wall rocks at Steamboat Springs, described in detail by Schoen et al., are believed to have been caused by a large convecting cell of thermal waters, meteoric in origin, that circulated primarily along fractures. Surficially altered basaltic andesites exhibit the following zonation of minerals from the present surface downward (Schoen et al., 1974):

- 0 - 111' opal and residual quartz, in approximately equal amounts
- 68 - 170' 3% of rock is pyrite
- 111' top of water table; just below

this, alunite becomes abundant
 111 -114' amorphous opal fills all open
 spaces, producing a dense rock
 below 120' alunite diminishes, kaolinite
 increases
 below 132' alunite is gone, rock consists of
 montmorillonite, decreasing
 kaolinite, illite, residual
 quartz, orthoclase, plagioclase,
 and minor biotite
 below 133' effect of hypogene alteration
 predominates over that of
 surficial alteration
 below 170' < 1% of rock is pyrite

Surficially altered rocks occur only where the thermal
 water table does not intersect the surface, and are
 believed to be due to descending, rather than ascending,
 fluids (Schoen et al., 1974). H_2S exsolves from the
 thermal waters at depth, rises towards the surface, and
 oxidizes into H_2SO_4 above the water table (Schoen et al.,
 1974). The H_2SO_4 trickles downward and outward, causing an
 "acid attack" in its path of travel, and creates the
 surficially altered rocks. Eventually, the water table is
 encountered, and H_2SO_4 breaks down into H^+ , HSO_4^- , and
 SO_4^{-2} .

Because of mineralogic similarities between the

surficial alteration at Steamboat Springs (Schoen et al., 1974) and the alteration associated with the Red Top structures, it is likely that both were caused by similar phenomena. Accordingly, at the Gooseberry mine, the near-neutral fluids at depth exsolved H_2S -rich gases that rose to the surface, oxidized to H_2SO_4 , and trickled downward. These fluids, now strongly acidic, altered the rocks above the water table to opal and residual quartz; the rocks at and just below the water table were altered to alunite, dickite, and some form of silica. The opal and residual quartz zone at the Gooseberry mine has since been eroded away.

The dickite-silica assemblage is similar to the kaolinite assemblage that occurs just below the water table at Steamboat Springs (Schoen et al., 1974). Alunite also occurs just below the water table at Steamboat Springs. It decreases in amount with depth, and disappears completely 21 feet below the present-day water table (Schoen et al., 1974). The dickite-silica assemblage is associated with the Red Top structures west of Steamboat Springs. The present-day paleowater table in the vicinity of Steamboat Springs

DISCUSSION

The alteration surrounding the Gooseberry vein was, in all likelihood, caused by the same hydrothermal event as the alteration enveloping the Red Top structures; this implies that both fault sets were open to the mineralizing fluids. The difference between the alteration assemblages observed in the two locations is believed by this author to be due to two different levels of exposure of the system. Accordingly, if mineralization does occur along the Red Top structures, it is expected to be at a greater depth below the present surface than that of the Gooseberry vein, because the altered rocks at the surface along the Red Top structures are believed to represent a higher level of exposure in the system than those along the Gooseberry vein. Figure 12 is an interpretive cross section of the alteration types observed at the Gooseberry mine.

The dickite-silica assemblage is similar to the kaolinite assemblage that occurs just below the water table at Steamboat Springs (Schoen et al., 1974). Alunite also occurs just below the water table at Steamboat Springs. It decreases in amount with depth, then disappears completely 21 feet below the present-day water table (Schoen et al., 1974). The dickite-silica assemblage associated with the Red Top structure west probably formed just below the paleowater table (note the presence of alunite here)

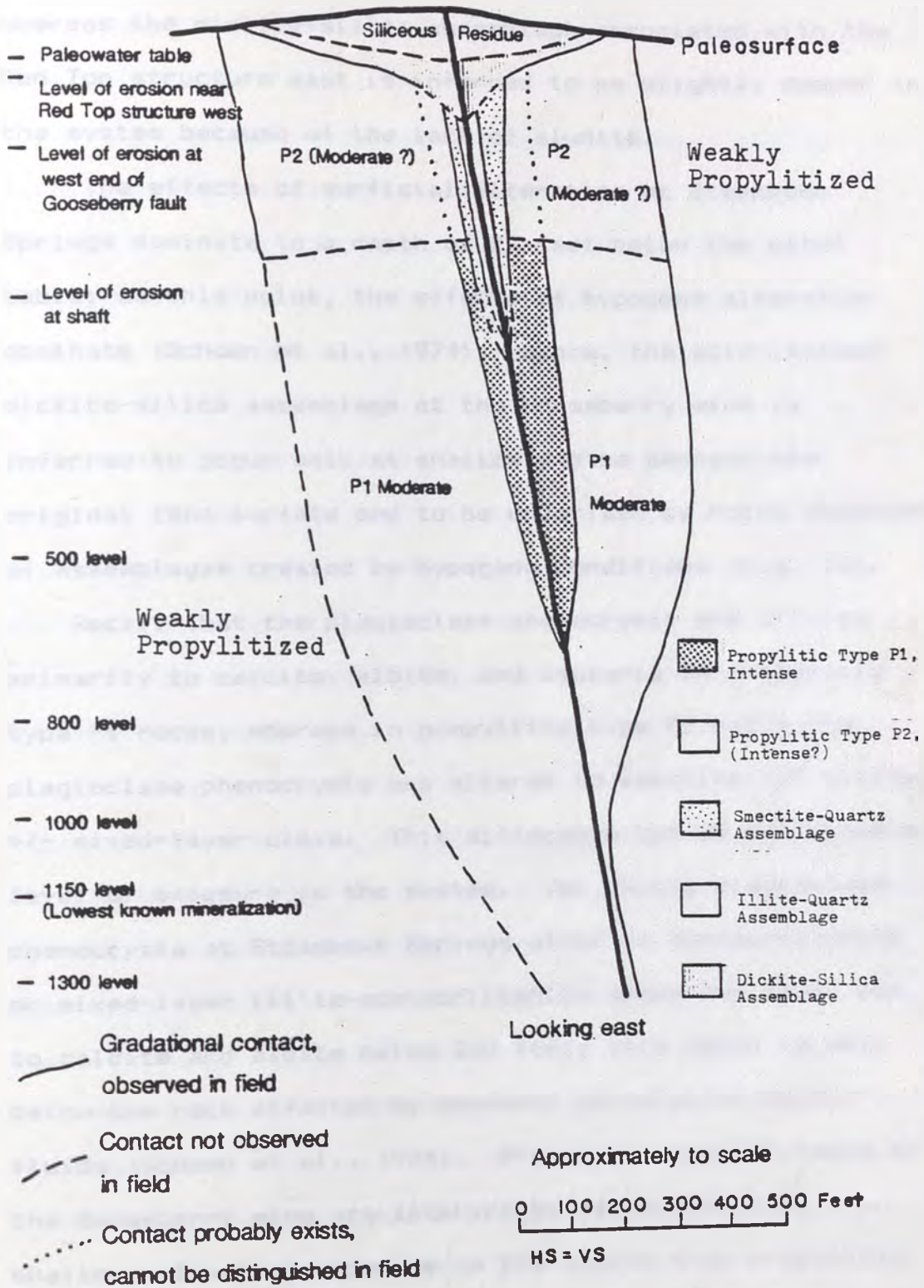


Fig. 12. Interpretive cross section showing the alteration types present at the Gooseberry mine (modified from Buchanan, 1981).

whereas the dickite-silica assemblage associated with the Red Top structure east is inferred to be slightly deeper in the system because of the lack of alunite.

The effects of surficial alteration at Steamboat Springs dominate to a depth of 22 feet below the water table; at this point, the effects of hypogene alteration dominate (Schoen et al., 1974). Hence, the acid-leached dickite-silica assemblage at the Gooseberry mine is inferred to occur only at shallow depths beneath the original land surface and to be underlain by rocks composed of assemblages created by hypogene conditions (Fig. 12).

Recall that the plagioclase phenocrysts are altered primarily to calcite, albite, and adularia in propylitic type P1 rocks, whereas in propylitic type P2 rocks the plagioclase phenocrysts are altered to smectite +/- illite +/- mixed-layer clays. This difference can be explained by level of exposure in the system. The calcic plagioclase phenocrysts at Steamboat Springs alter to montmorillonite or mixed-layer illite-montmorillonite above 200 feet, but to calcite and albite below 200 feet; this depth is well below the rock affected by downward percolating acidic fluids (Schoen et al., 1974). Propylitic type P2 rocks at the Gooseberry mine are interpreted as representing a shallower level of exposure in the system than propylitic type P1 rocks. Figure 12 shows the P1-P2 contact as roughly horizontal; this attitude best fits the observed

outcrops of propylitized rock along the Gooseberry fault (Plate II).

At other epithermal vein-type deposits, a low pH assemblage consisting of alunite, sericite, illite, kaolinite, and/or montmorillonite is often located above ore shoots (Buchanan, 1981). This cannot be proven conclusively at the Gooseberry mine by this study. The western limit of the central ore shoot (Plate IXb) roughly correlates with the smectite-quartz assemblage near specimen GS-66 (Plate II). Unfortunately, the lack of exposure overlying the rest of this high-grade zone prevents observation of the altered rocks. The relationship between the easternmost ore shoot (Plate IXb) and the alteration type of the overlying rocks is unknown due to alluvial cover. The ore shoot to the west (Plate IXb) underlies an area of very poor surface exposure (Plate II); here again, the relationship is uncertain. The gypsum pit area, an excellent example of the smectite-quartz assemblage, is located to the west of the existing workings.

The two north-northeast trending fault zones that cut the Gooseberry fault are spatially associated with low pH-assemblage rocks along the Gooseberry fault (Plate II). The easternmost occurrence is discussed above, and is spatially related to an ore shoot. The westernmost fault zone does intersect the old 1000 level, but none of the

other levels extend this far to the west. Any relationship between this fault zone and ore-grade material cannot be determined without further underground exploration. Perhaps these cross faults assisted in localizing the precious-metal mineralization. Further work in this direction could produce a valuable guide to ore.

The relationship between low pH-assemblage rocks and mineralization at depth should be tested by drilling. Additionally, an exploratory crosscut could be driven from the 1000 level at approximately 250,100E to the north, if economically feasible; this would evaluate the parallel structure to the north in the area underlying the zone of smectite-quartz- and illite-quartz-assemblage rocks (Plate II). If these areas of low pH-assemblage rocks do prove related to mineralization at depth, all such zones should be evaluated thoroughly. Trenching should be done in areas lacking outcrop to expose any concealed low pH- assemblage rocks.

The Gooseberry mine appears to have excellent potential for expansion, both along the Gooseberry fault to the west and along the parallel structure to the north. In addition, the Red Top structures may also host mineralization, and therefore warrant further examination.

APPENDICES

APPENDIX A: FIELD TECHNIQUES

Surface and underground mapping at the Gooseberry mine began in early June, 1983, and was completed by early August, 1983; 414 samples were collected. Approximately 30 days were spent working on the surface; 172 rock samples were taken. A 1:600 scale topographic map was employed as a base map in the vicinity of the Gooseberry fault zone and a 1:1200 scale topographic base map was utilized for the remainder of the study area.

Approximately 15 days were required to map the underground workings; 183 samples were collected. In addition, 51 samples from 13 core holes provided access to wall rock unexposed by crosscuts. Only the new 500, 800, 1000, 1150, and 1300 levels, as well as parts of the old 100, 200, and 400 levels, were accessible. The Gooseberry mine staff provided a 1:240 scale geology map of these levels for use as a base map.

Due to stope access restrictions imposed by the Gooseberry mine staff, only one-half day was allowed to collect grab samples of the vein for fluid-inclusion work; eight sites were sampled.

APPENDIX B: X-RAY EQUIPMENT AND SAMPLE PREPARATION

METHODS

Whole-rock samples were prepared for X-ray analysis by pulverizing in a steel percussion mortar, followed by hand-grinding with a mortar and pestle. Acetone was added to the ground sample and the slurry was poured onto a glass slide. A total of 318 whole-rock samples were scanned from four degrees to 50 degrees two theta on a Norelco diffractometer at a speed of two degrees per minute and a chart speed of a half inch per minute.

Forty-one samples were chosen for glycolation. A sufficient amount of a 1:1 glycol-to-water mixture was added to the prepared whole rock slide to visibly moisten the sample. After air-drying overnight, the slide was re-X-rayed. This technique proved the presence of the smectite group and of mixed-layer clays.

APPENDIX C: SELECTED THIN-SECTION AND X-RAY DIFFRACTION

DATA

A total of 80 samples were prepared for thin-section study, 34 from underground, 46 from the surface. Specimens were chosen because the sample was representative of a particular alteration assemblage or because the X-ray diffraction pattern, combined with the field description,

was insufficient to assign the rock to an alteration assemblage.

Eighty-six grain mounts were prepared to look for epidote and/or clinozoisite; these minerals occur in insufficient quantities to be identified by X-ray diffraction techniques.

X-ray diffraction techniques were utilized to identify the clay minerals. Kaolinite and dickite have X-ray diffraction patterns that are very similar. The dickite pattern generally exhibits two peaks that the kaolinite pattern does not; these two peaks occur at 21.55 and 35.77 degrees two theta (Joint Committee on Powder Diffraction Standards, 1980). At the Gooseberry mine, the kandite minerals that were called dickite exhibited strong, sharp peaks at both of these two theta values.

The following table lists the alteration minerals from selected thin sections and X-ray diffraction runs.

Selected Thin Section and X-Ray Diffraction Data

Sample no.	Albite	Adularia	Chlorite	Smectite	Illite	Mixed layer clays	Dickite	Calcite	Epidote group	Zeolite group	Pyrite	Alunite	Quartz	Cristobalite	Opal	Alteration assemblage
GU-266	x	x	x	x	x				x		x					P1 I
GU-260	x	x	x	x	x			x	x		x					P1
GU-270	x	x	x	x					x		x					P1
GU-258	x	x	x	x				x			x					P1
GU-226	x	x	x	x				x	x		x					P1
GU-245	x	x	x	x				x	x		x					P1
GU-157	x	x	x	x	x			x	x							WP
GU-202	x	x	x	x				x	x		x					P1
GU-141	x	x	x	x				x	x							WP
GU-123	x	x	x	x	x	x		x	x							P1
GU-140	x	x	x	x				x	x		x					P1
GU-273	x	x	x	x				x	x							WP
GU-271	x	x	x	x				x	x	x						P1
GS- 7			x	x				x	x		x					WP
GS- 31	x	x	x	x	x			x	x							P1
GS- 19				x	x					x						P2
GS-254				x	x											P2
GS-307				x		x										P2
GS-295			x	x	x			x	x							P2
GS- 59				x	x						x					M

Selected Thin Section and X-Ray Diffraction Data (cont.)

Sample no.	Albite	Adularia	Chlorite	Smectite	Illite	Mixed layer clays	Dickite	Calcite	Epidote group	Zeolite group	Pyrite	Alunite	Quartz	Cristobalite	Opal	Alteration assemblage
GS-335				x	x											M
GS- 64					x											H
GS-321							x						x			D
GS-322							x					x	x		x	D
GS-325							x					x		x		D
GS-339							x						x			D

The GU series is from underground; sample locations are given on Plate III. The GS series is from the surface; sample locations are given on Plate II. P1I = propylitic assemblage P1, intense; P1 = propylitic assemblage P1; WP = weakly propylitized; P2 = propylitic assemblage P2; M = smectite-quartz-illite assemblage; I = illite-quartz assemblage; D = dickite-silica assemblage; see text for explanation. x indicates the presence of that mineral.

APPENDIX D: METHODS UTILIZED IN CONSTRUCTING THE
STRUCTURE CONTOUR PROJECTION AND
ACCOMPANYING OVERLAYS

The longitudinal projection of the reconstructed Gooseberry vein showing structure contours was constructed from 1:240 scale geology maps of the 100, 500, 600, 700, 800, 900, and 1000 levels, provided by the Gooseberry mine staff, that showed the location and attitude of the veins and faults. Because the Gooseberry vein has undergone post-mineralization offset, it was necessary to reconstruct the vein prior to post-mineralization faulting. The amount of movement along the post-mineral faults is unknown. As an approximation, the strike-slip component of motion was removed from each cross fault by lining up the footwall side of the vein across each cross fault. A 1:240 scale plan view of the reconstructed vein was thus created for each level. The vein does not crop out at the surface; therefore, the highest level shown on the structure contour map is the 100 level.

The attitude of the reference plane was assigned in the following manner: the dip was calculated by taking the arithmetic average of all mapped vein dips; the strike was calculated by taking the arithmetic average of the various vein strikes from the reconstructed level maps. The resulting attitude is $N72^{\circ}W, 80^{\circ}S$.

A vertical zero plane was chosen to coincide with the E251,100 coordinate line; this plane intersects all of the levels. The point of intersection between the vertical zero plane and the reference plane at the plane of any given level is the zero point for that level. Data points were chosen at 50 foot intervals along the reference plane from the zero point for each level, creating a grid of data points on the reference plane.

The reference plane was placed arbitrarily in the footwall so as to not intersect the vein. For each data point, a perpendicular line was drawn from the reference plane to the center of the vein (Conolly, 1936); the resulting distance in feet was noted. The data points were plotted at a scale of 1:1200 and the distances were contoured, producing Plate V. Note that a different reference plane would produce a different contour map, but that the indicated trends would be similar (Conolly, 1936).

The same data points were utilized in constructing Plate VII, the longitudinal projection of the reconstructed Gooseberry vein showing vein thickness contours. Vein thickness was obtained from the level maps for each data point, plotted on the reference plane grid, and contoured.

Asamera Minerals (U.S.) Inc. supplied gold and silver vein assay data for the new 500, old 600, old 700, new 800, old 900, and old 1000 levels; stope assay data was not available. The same data points used in constructing the

structure contour and vein thickness projections were utilized. However, instead of taking just the assay values available for a given data point, the values from 20 feet on each side of the data point were incorporated. A weighted average, weighted according to sample thickness, was calculated for each data point and contoured. The original sample spacing is inconsistent; therefore, the weighted averages are calculated from a varying number of samples. A built-in assumption here is that the level assay data is accurate, and that it adequately represents the precious-metal content near that point in the vein.

The longitudinal projection of the reconstructed Gooseberry vein showing silver-to-gold ratio contours was constructed by dividing the calculated silver value by the calculated gold value for a given data point and contouring the result.

The longitudinal projection of the reconstructed Gooseberry vein showing equivalent-silver-foot contours was constructed in March, 1985, and reflects the price of gold (\$289.60/oz) and silver (\$5.69/oz) at that time. The calculated gold grade was multiplied by 51 (gold price divided by silver price) to convert to equivalent silver value and was added to the calculated silver value, yielding total equivalent silver content. The equivalent silver content was multiplied by the vein thickness at that point, yielding a result in ounce-feet per ton.

APPENDIX E: HEATING-FREEZING EQUIPMENT AND FLUID-
INCLUSION SAMPLE PREPARATION METHODS

Doubly polished plates for fluid-inclusion study were prepared according to the method recommended by Roedder (1984). Coarser-grained vein material was ground flat, cut to size, and cemented to an epoxy-filled mount with Duco Cement, an acetone-soluble cement. The chip was cut to approximately 3 millimeters in width with a standard diamond trim saw. Approximately one millimeter was then ground off on a lap using 200 grit. Progressively finer grit (400, then 600) was employed to remove any scratches. Final polishing was accomplished using 6, 3, and 1 micron polishing compound, successively. This procedure was repeated on the second side, resulting in a doubly polished chip approximately one millimeter in thickness.

Bruha (1983) describes in detail the heating-freezing stage and calibration procedures utilized for the fluid inclusion work. A model 3 Roman Science microscope stage is mounted on a Leitz binocular/monocular microscope equipped with long working-distance objectives. Maximum attainable temperature is greater than 500°C ; minimum is approximately -100°C .

All eight of the fluid-inclusion samples were prepared; several of them were prepared twice because of the softness of the calcite. Three of the fluid-inclusion

samples contained primary inclusions that all showed evidence of cracking; a fourth contained only one non-cracked primary inclusion; and a fifth was too fine-grained to use. Thus, homogenization temperatures could only be measured for three fluid inclusion samples.

APPENDIX F: GAS ANALYSIS EQUIPMENT AND SAMPLE PREPARATION METHODS

Each sample was crushed in a steel percussion mortar. Approximately one gram of sample between 70 and 100 mesh was separated via sieve and shipped to Exploration Research Laboratories, Salt Lake City, Utah. Two grams of FI-6 were separated, divided in half, and labeled 6 and 9. Three to four grams of FI-4 were sieved. One gram was labeled 4; this is a quartz-calcite mixture. The remainder was mixed with dilute HCl until all the calcite was dissolved. The residual quartz was thoroughly rinsed with distilled water, air dried overnight, and labeled 10.

The laboratory procedure utilized is described by Bruha (1983). A small amount of sample is placed in a vial flushed with helium. The sample is heated to 425°C, causing the inclusions to decrepitate. All released gases are drawn off by syringe and injected into a gas chromatograph/mass spectrometer for analysis; the detection limit is approximately 50 ppb. This particular method can

not analyze for H_2O , and therefore is not quantitative.

APPENDIX G: SAMPLE CALCULATIONS

Total Carbon Versus Total Sulfur

$$\begin{aligned} \text{Total C} = & 0.75(CH_4) + 0.80(C_2H_6) + 0.82(C_3H_8) \\ & + 0.273(CO_2) + 0.23(CS_2) + 0.20(COS) \end{aligned}$$

$$\begin{aligned} \text{Total S} = & 0.94(H_2S) + 0.50(SO_2) + 0.77(CS_2) \\ & + 0.53(COS) \end{aligned}$$

Total Oxidized Carbon Plus Sulfur Versus Total Reduced Carbon Plus Sulfur

$$\begin{aligned} \text{Total oxidized (C + S)} = & 0.273(CO_2) + 0.73(COS) \\ & + 0.50(SO_2) \end{aligned}$$

$$\begin{aligned} \text{Total reduced (C + S)} = & 0.75(CH_4) + 0.80(C_2H_6) \\ & + 0.82(C_3H_8) + 0.94(H_2S) \\ & + 1.0(CS_2) \end{aligned}$$

The above equations were provided by Exploration Research Laboratories.

Mole Fraction of Carbon Dioxide Present

The mole fraction of component x in a solution is defined as the number of moles of x divided by the total number of moles of all the components in the solution. Utilizing this definition in conjunction with the following assumptions and the gas analyses yields a rough estimate of the CO₂ content:

1. The fluid inclusion is 98 weight percent, or more, H₂O (see Gas Analyses section, in text)
2. the relative gas proportions from the gas analyses are correct
3. the fluid is composed solely of H₂O and the analyzed gases.

The accuracy of the CO₂ estimate depends upon how closely these assumptions approach reality. The following equation was utilized to calculate the mole fraction of CO₂:

$$\text{Mole fraction CO}_2 = \frac{[\text{CO}_2/44]}{[(\text{H}_2\text{O}/18) + (\text{CO}_2/44)]}$$

The other gases occur in such small amounts that their effect on this calculation is negligible. The mole fraction of CO₂ was also calculated assuming that the fluid inclusion was 99 and 99.5 weight percent H₂O.

REFERENCES

- Anonymous, 1983, Gooseberry Mine, Asamera Minerals (US) Inc.: Unpub. brochure, 10 p.
- Asamera Inc., 1984, Annual report to the stockholders, 55 p.
- Bingler, E. C., 1973, Oligocene welded tuff sequence in northern Wassuk Range, central-western Nevada: Geol. Soc. America Abs. with Programs, v. 5, p. 12.
- Bingler, E. C., 1978, Abandonment of the name Hartford Hill Rhyolite Tuff and adoption of new formation names for middle Tertiary ash-flow tuffs in the Carson City-Silver City area, Nevada: U.S. Geol. Survey Bull. 1457-D, p. D1-D19.
- Bodnar, R. J., and Kuehn, C. A., unpub. manuscript, (early 1980's), Effect of dissolved carbon dioxide on the estimated depths of formation of epithermal gold-silver deposits as calculated from fluid inclusion data: 38 p., 11 figures.
- Bonham, H. F., 1969, Geology and mineral deposits of Washoe and Storey Counties, Nevada: Nevada Bureau of Mines and Geology, Bull. 70, 140 p.
- ✓ Bruha, D. J., 1983, Paragenetic and fluid-inclusion study of Pb-Zn-Ag mineralization at Mina Teresita, Huachocolpa District, Peru: Unpub. M.S. thesis, Univ. of Nevada, Reno, 55 p.
- Buchanan, L. J., 1979, The Las Torres Mine, Guanajuato, Mexico - Ore controls of a fossil geothermal system: Unpub. Ph.D. thesis, Colorado School of Mines, 138 p.
- Buchanan, L. J., 1980, Ore controls of vertically stacked deposits, Guanajuato, Mexico: Soc. Min. Eng. AIME, preprint no. 80-82, 26 p.
- Buchanan, L. J., 1981, Precious metal deposits associated with volcanic environments in the southwest, in Dickinson, W. R., and Payne, W. D., eds., Relations of Tectonics to Ore Deposits in the Southern Cordillera: Arizona Geological Society Digest, v. XIV, p. 237-262.
- Casadevall, T., and Ohmoto, H., 1977, Sunnyside mine, Eureka mining district, San Juan County, Colorado:

- Geochemistry of gold and base metal ore deposition in a volcanic environment: *Econ. Geol.*, v. 72, p. 1285-1320.
- Clifton, C. G., Buchanan, L. J., and Durning, W. P., 1980, Exploration procedure and controls of mineralization in the Oatman Mining District, Oatman, Arizona: *Soc. Min. Eng. AIME*, Preprint no. 80-143, 17 p.
- Conolly, H. J. C., 1936, A contour method of revealing some ore structures: *Econ. Geol.*, v. 31, p. 259-271.
- Dalrymple, G. B., 1979, Critical tables for conversion of K-Ar ages from old to new constants: *Geology*, v. 7, p. 558-560.
- Ellis, A. J., 1979, Explored geothermal systems, in Barnes, H. L., ed., *Geochemistry of Hydrothermal Ore Deposits*: New York, Wiley-Interscience, p. 632-683.
- Ellis, A. J., and Golding, R. M., 1963, The solubility of carbon dioxide at greater than 100 degrees centigrade in water and in sodium chloride solutions: *Am. Jour. Sci.*, v. 261, p. 47-60.
- ✓ Fahley, M. P., 1981, Fluid inclusion study of the Tonopah district, Nevada: Unpub. M.S. thesis, Colorado School of Mines, 106 p.
- Giggenbach, W. F., 1984, Mass transfer in hydrothermal alteration systems - a conceptual approach: *Geochimica et Cosmochimica Acta*, v. 48, p. 2693-2711.
- Goodell, P. C., and Petersen, U., 1974, Julcani mining district, Peru: A study of metal ratios: *Econ. Geol.*, v. 69, p. 347-361.
- Grim, R. A., 1968, *Clay mineralogy*, Second Edition: McGraw-Hill Book Co., New York, 596 p.
- Haas, J. L., 1971, The effect of salinity on the maximum thermal gradient of a hydrothermal system at hydrostatic pressure: *Econ. Geol.*, v. 66, p. 940-946.
- Haas, J. L., 1976, Physical properties of the coexisting phases and thermochemical properties of the H₂O component in boiling NaCl solutions: *U.S. Geol. Survey Bull.* 1421-A, 73 p.
- Hardyman, R. F., unpub. report, (between 1974 and 1976), *Geologic investigations of the Gooseberry-Ramsey mining districts, Storey County, Nevada*: prepared for

APCO Oil Corp., 20 p.

Hemley, J. J., and Jones, W. R., 1964, Chemical aspects of hydrothermal alteration with emphasis on hydrogen metasomatism: *Econ. Geol.*, v. 59, p. 538-569.

Henley, R. W., and Ellis, A. J., 1983, Geothermal systems ancient and modern: A geochemical review: *Earth Science Reviews*, v. 19, p. 1-50.

Henley, R. W., Truesdell, A. H., and Barton, P. B. Jr., 1984, Fluid-mineral equilibria in hydrothermal systems: *Reviews in Economic Geology*, v. 1, 267 p.

Holland, H. D., and Malinin, S. D., 1979, The solubility and occurrence of non-ore minerals, in Barnes, H. L., ed., *Geochemistry of Hydrothermal Ore Deposits*: New York, Wiley-Interscience, p. 461-508.

Hudson, D., 1984a, Geology of the Comstock District, Storey County, Nevada, prepared for United Mining Company of Nevada, Virginia City, Nevada: on file at the Nevada Bureau of Mines and Geology, Mining District Files, File no. 309.

Hudson, D., 1984b, Geology of the Steamboat Springs - Virginia City region, Nevada, in Johnson, J. L., ed., *Exploration for ore deposits of the North American cordillera: Symposium of the Association of Exploration Geochemists, Reno, Nevada, Field Trip Guidebook, Field Trip 11.*

Joint Committee on Powder Diffraction Standards, 1980, *Mineral Powder Diffraction File Data Book*: International Center for Diffraction Data, Swarthmore, Pennsylvania, 1168 p.

Kamilli, R. J., and Ohmoto, H., 1977, Paragenesis, zoning, fluid inclusion, and isotope studies of the Finlandia vein, Colqui District, central Peru: *Econ. Geol.*, v. 72, p. 950-982.

Kemp, W. R., 1976, Thin section and polished section descriptions - Gooseberry Mine: prepared for Scurry Rainbow Oil, Reno, Nevada, unpub., unpaginated.

Kleeberger, S. R., unpub. report, (between 1974-1976), Gooseberry mine thin and polished section data: 19 p.

Meyer, C., and Hemley, J. J., 1967, Wall rock alteration, in Barnes, H. L., ed., *Geochemistry of hydrothermal ore deposits*: Holt, Rinehart, and Winston, Inc., New

- York, p. 166-235.
- Moore, J. G., 1969, Geology and mineral deposits of Lyon, Douglas, and Ormsby Counties, Nevada: Nevada Bureau Mines and Geology, Bull. 75, 43 p.
- Morton, J. L., Silberman, M. L., Bonham, H. F., Garside, L. J., and Noble, D. C., 1977, K-Ar ages of volcanic rocks, plutonic rocks, and ore deposits in Nevada and eastern California - Determinations run under the USGS-NBMG Cooperative Program: Isochron/West, v. 20, p. 19-29.
- Nash, J. T., 1972, Fluid-inclusion studies of some gold deposits in Nevada: U.S. Geol. Survey Prof. Paper 800-C, p. C-15-C-19.
- ✓ Nolan, T. B., 1935, The underground geology of the Tonopah mining district, Nevada: Nevada Bureau of Mines and Geology, Bull. 23, 49 p.
- O'Neil, J. R., Silberman, M. L., Fabbi, B. P., and Chesterman, C. W., 1973, Stable isotope and chemical relations during mineralization in the Bodie mining district, Mono County, California: Econ. Geol., v. 68, p. 765-784.
- ✓ Osborne, M. A., 1985, Alteration and mineralization of the northern half of the Aurora mining district, Mineral County, Nevada: Unpub. M.S. thesis, Univ. of Nevada, Reno, 93p.
- Petersen, U., Noble, C. C., Arenas, M. J., and Goodell, P. C., 1977, Geology of the Julcani mining district, Peru: Econ. Geol., v. 72, p. 931-949.
- Potter, R. W., 1977, Pressure corrections for fluid-inclusion homogenization temperatures based on the volumetric properties of the system NaCl-H₂O: Jour. Research U.S. Geol. Survey, v. 5, p. 603-607.
- ✓ Proffett, J. M. Jr., and Proffett, B., 1976, Stratigraphy of the Tertiary ash-flow tuffs in the Yerington district, Nevada: Nevada Bureau Mines and Geology Report 27, 28 p.
- Roedder, E., 1984, Fluid Inclusions: Reviews in Mineralogy, v. 12, 644 p.
- Rose, R. L., 1969, Geology of parts of the Wadsworth and Churchill Butte Quadrangles, Nevada: Nevada Bureau of Mines and Geology Bull. 71, 27 p.

- Ross, C. S., and Kerr, P. F., 1930, The kaolin minerals: U.S. Geol. Survey Prof. Paper 165-E, p. 151-176.
- Royse, S., in preparation, Geochemical study of the Gooseberry mine area, Storey County, Nevada: Unpub. M.S. thesis, Univ. of Nevada, Reno.
- Sawkins, F. J., O'Neil, J. R., and Thompson, J. M., 1979, Fluid inclusion and geochemical studies of vein gold deposits, Baguio district, Philippines: Econ. Geol., v. 74, p. 1420-1434.
- Schafer, R. W., 1976, The mineralogy, structure, and alteration pattern of the Gooseberry mine, Storey County, Nevada: Unpub. M.S. thesis, Miami Univ., Oxford, Ohio, 79 p.
- Schoen, R., White, D. E., and Hemley, J. J., 1974, Argillization by descending acid at Steamboat Springs, Nevada: Clays and Clay Mineralogy, v. 22, p. 1-22.
- Silberman, M. L., and McKee, E. H., 1972, A summary of radiometric age determinations on Tertiary volcanic rocks from Nevada and eastern California: Part II, western Nevada: Isochron/West, v. 4, p. 7-28.
- Smith, D. M. Jr., Albinson, T., and Sawkins, F. J., 1982, Geologic and fluid inclusion studies of the Tayoltita silver-gold vein deposit, Durango, Mexico: Econ. Geol., v. 77, p. 1120-1145.
- Srodon, J., and Eberl, D. D., 1984, Illite, in Bailey, S. W., ed., Micas: Reviews in Mineralogy, v. 13, p. 495-575.
- Stewart, J. H., 1980, Geology of Nevada - A discussion to accompany the geologic map of Nevada: Nevada Bureau of Mines and Geology Special Publication No. 4, 136 p.
- Takenouchi, S., and Kennedy, G. C., 1965, The solubility of carbon dioxide in NaCl solutions at high temperatures and pressures: Amer. Jour. Sci., v. 263, p. 445-454.
- Vikre, P. G., 1985, Precious metal vein systems in the National district, Humboldt County, Nevada: Econ. Geol., v. 80, p. 360-393.
- Wallace, A. B., 1975, Geology and mineral deposits of the Pyramid district, southern Washoe County, Nevada: Unpub. Ph.D. thesis, Univ. of Nevada, Reno, 162 p.

White, D. E., 1981, Active geothermal systems and hydrothermal ore deposits, in Skinner, B. J., ed., Econ. Geol. Seventy-fifth Anniversary Volume: p. 329-423.

Zerwick, S. A., 1982, The analysis of adsorbed gases from alteration minerals as a potential exploration tool for epithermal vein deposits: Unpub. M.S. thesis, Univ. Minnesota, 85 p.